TTI-2-5-85-405-1

TEXAS
TRANSPORTATION
INSTITUTE

STATE DEPARTMENT
OF HIGHWAYS AND
PUBLIC TRANSPORTATION

COOPERATIVE
RESEARCH

THE EFFECTS OF EMBEDMENT DEPTH, SOIL PROPERTIES, AND POST TYPE ON THE PERFORMANCE OF HIGHWAY GUARDRAIL POST

in cooperation with the
Department of Transportation
Federal Highway Administration

RESEARCH REPORT 405-1
STUDY 2-5-85-405
HIGHWAY GUARDRAILS

TECHNICAL REPORT STANDARD TITLE PAGE

1. Report No.	2. Government Accession No.	3. Recipient's Catalog No.
FHWA/TX-86/64+405-1		

4. Title and Subtitle

THE EFFECTS OF EMBEDMENT DEPTH, SOIL PROPERTIES, AND POST TYPE ON THE PERFORMANCE OF HIGHWAY GUARDRAIL POST

5. Report Date

August 1986

6. Performing Organization Code

7. Author(s)

David W. Eggers and T. J. Hirsch

8. Performing Organization Report No.

Research Report 405-1

9. Performing Organization Name and Address

Texas Transportation Institute
The Texas A&M University System
College Station, Texas 77843

10. Work Unit No.

11. Contract or Grant No.

Study No. 2-5-85-405

12. Sponsoring Agency Name and Address

Texas State Department of Highways and Public Transportation; Transportation Planning Division
P.O. Box 5051
Austin, Texas 78763

13. Type of Report and Period Covered

Interim - September 1984 - August 1986

14. Sponsoring Agency Code

15. Supplementary Notes

Research performed in cooperation with DOT, FHWA.
Research Study Title: Guardrail on Low Fill Bridge Length Culverts

16. Abstract

The Texas State Department of Highways and Public Transportation (TSDHPT) currently uses two types of guardrail posts: (1) a circular wood post and (2) a steel W6 x 8.5 post. The current specifications require that the post must have a minimum soil embedment depth of 38 in. When a guardrail system is required at a culvert, SDHPT currently requires a rigid bridge rail when the full embedment depth of 38 in. cannot be achieved. The objective of this research study was to determine if the current guardrail design could be modified to achieve the necessary strength when full post embedment could not be achieved. The purpose of this report was to assess the effects of post type, soil conditions, and embedment depth on the load-deformation characteristics of the guardrail post. With this information, it is believed that a successful guardrail can be designed using more post with less than the full 38 in. embedment. Posts with only 18 in. or 24 in. embedment could be used at 3 ft-1 1/2 in. spacing and still produce the required strength for example.

A series of static load tests were conducted on timber and steel posts embedded 18 in., 24 in., 30 in., and 38 in. in two different soils to determine the effects of post type, soil conditions, and embedment depth on the amount of energy dissipated by the soil. The results of these field tests were used to verify a mathematical model which could be used to predict guardrail post load capacity.

17. Key Words	18. Distribution Statement
Embedment Depth, Soil Properties, Post Types, Static Load Tests	No restrictions. This document is made available to the public through the National Technical Information Service 5285 Port Royal Road Springfield, Virginia 22161

19. Security Classif. (of this report)	20. Security Classif. (of this page)	21. No. of Pages	22. Price
Unclassified	Unclassified	60	

Form DOT F 1700.7 (8-69)

THE EFFECTS OF EMBEDMENT DEPTH, SOIL PROPERTIES, AND POST TYPE ON THE PERFORMANCE OF HIGHWAY GUARDRAIL POST

by

David W. Eggers
Research Assistant

and

T. J. Hirsch
Research Engineer

Research Report 405-1
on
Research Study No. 2-5-85-405
Guardrail on Low Fill Bridge Length Culverts

Sponsored by

Texas State Department of Highways and Public Transportation
in cooperation with
the U.S. Department of Transportation
Federal Highway Administration

August 1986

Texas Transportation Institute
The Texas A&M University System
College Station, Texas 77843

METRIC CONVERSION FACTORS

Approximate Conversions to Metric Measures

Symbol	When You Know	Multiply by	To Find	Symbol
		LENGTH		
in	inches	*2.5	centimeters	cm
ft	feet	30	centimeters	cm
yd	yards	0.9	meters	m
mi	miles	1.6	kilometers	km
		AREA		
in^2	square inches	6.5	square centimeters	cm^2
ft^2	square feet	0.09	square meters	m^2
yd^2	square yards	0.8	square meters	m^2
mi^2	square miles	2.6	square kilometers	km^2
	acres	0.4	hectares	ha
		MASS (weight)		
oz	ounces	28	grams	g
lb	pounds	0.45	kilograms	kg
	short tons (2000 lb)	0.9	tonnes	t
		VOLUME		
tsp	teaspoons	5	milliliters	ml
Tbsp	tablespoons	15	milliliters	ml
fl oz	fluid ounces	30	milliliters	ml
c	cups	0.24	liters	l
pt	pints	0.47	liters	l
qt	quarts	0.95	liters	l
gal	gallons	3.8	liters	l
ft^3	cubic feet	0.03	cubic meters	m^3
yd^3	cubic yards	0.76	cubic meters	m^3
		TEMPERATURE (exact)		
°F	Fahrenheit temperature	5/9 (after subtracting 32)	Celsius temperature	°C

*1 in = 2.54 (exactly). For other exact conversions and more detailed tables, see NBS Misc. Publ. 286, Units of Weights and Measures, Price $2.25, SD Catalog No. C13.10:286.

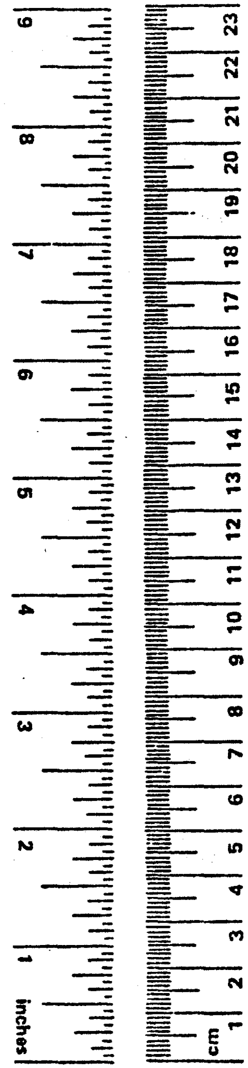

Approximate Conversions from Metric Measures

Symbol	When You Know	Multiply by	To Find	Symbol
		LENGTH		
mm	millimeters	0.04	inches	in
cm	centimeters	0.4	inches	in
m	meters	3.3	feet	ft
m	meters	1.1	yards	yd
km	kilometers	0.6	miles	mi
		AREA		
cm^2	square centimeters	0.16	square inches	in^2
m^2	square meters	1.2	square yards	yd^2
km^2	square kilometers	0.4	square miles	mi^2
ha	hectares (10,000 m^2)	2.5	acres	
		MASS (weight)		
g	grams	0.035	ounces	oz
kg	kilograms	2.2	pounds	lb
t	tonnes (1000 kg)	1.1	short tons	
		VOLUME		
ml	milliliters	0.03	fluid ounces	fl oz
l	liters	2.1	pints	pt
l	liters	1.06	quarts	qt
l	liters	0.26	gallons	gal
m^3	cubic meters	35	cubic feet	ft^3
m^3	cubic meters	1.3	cubic yards	yd^3
		TEMPERATURE (exact)		
°C	Celsius temperature	9/5 (then add 32)	Fahrenheit temperature	°F

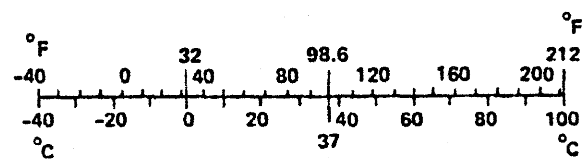

TABLE OF CONTENTS

	Page
INTRODUCTION	1
MATHEMATICAL MODEL	2
SOIL CONDITIONS	8
STATIC LOAD TESTS	16
INTRODUCTION	16
TESTING PROGRAM	16
PLACEMENT OF POST	16
EQUIPMENT AND INSTRUMENTATION	16
TEST PROCEDURE	22
RESULTS AND CONCLUSIONS	26
STATIC TEST RESULTS	26
COMPARISON OF TEST RESULTS WITH THEORETICAL PREDICTIONS	26
CONCLUSIONS	37
RECOMMENDATIONS FOR FURTHER RESEARCH	37
REFERENCES	38
APPENDIX A - SEQUENTIAL PHOTOGRAPHS FOR TESTS 5-16	39
APPENDIX B - SPECIFICATIONS FOR METAL BEAM GUARD FENCE	52

LIST OF FIGURES

Figure		Page
1	Brom's Ultimate Lateral Soil Resistance for Cohesive Soils	3
2	Brom's Ultimate Lateral Soil Resistance for Cohensionless Soils	4
3	Lateral Load vs. Embedment Depth for Analytical Model (Cohensionless Soils)	5
4	Lateral Load vs. Embedment Depth for Analytical Model (Cohesive Soils)	6
5	Test Site for Static Tests	9
6	Shearing Stress vs. Deflection for Two Different Normal Stresses	10
7	Shearing Stress vs. Normal Stress for Cohesive Soil	11
8	Gradation Curve for the Cohesionless Soil	14
9	Shear Strength of Rockfill Material from Large Triaxial Test	15
10	Location of Timber Posts 1-8	17
11	Placement of Timber Posts 1-8	18
12	Location of Steel Posts 9-16	19
13	Placement of Steel Posts 9-16	20
14	Static Testing System	23
15	Attachment of Force Transducer to Loading Bracket	24
16	Loading Bracket for Timber Post	25
17	Loading Bracket for Steel Post	25
18	Lateral Load vs. Deflection for Post Embedded 18 in.	27
19	Lateral Load vs. Deflection for Post Embedded 24 in.	28
20	Lateral Load vs. Deflection for Post Embedded 30 in.	29
21	Lateral Load vs. Deflection for Post Embedded 38 in.	30
22	Comparison of Analysis and Field Load Tests 1-4 and 9-12	31
23	Comparison of Analysis and Field Load Tests 5-8 and 13-16	32
24	Sequential Photographs for Test 5	40
25	Sequential Photographs for Test 6	41
26	Sequential Photographs for Test 7	42
27	Sequential Photographs for Test 8	43
28	Sequential Photographs for Test 9	44
29	Sequential Photographs for Test 10	45

LIST OF FIGURES (continued)

Figure		Page
30	Sequential Photographs for Test 11	46
31	Sequential Photographs for Test 12	47
32	Sequential Photographs for Test 13	48
33	Sequential Photographs for Test 14	49
34	Sequential Photographs for Test 15	50
35	Sequential Photographs for Test 16	51
36	Specifications for Metal Beam Guard Fence	53

LIST OF TABLES

Table		Page
1	Summary of Static Analysis	7
2	Propertis of the Soil	12
3	Summary of Tests	21
4	Summary of Results	33
5	Percent of Static Post Test with an Embedment Depth of 38 Inches	34
6	Comparison of Wood and Steel Guardrail Posts in Cohesive and Cohesionless Soil - Static and Impact Tests	35
7	Strength of Timber Guardrail Posts in Rock	36

INTRODUCTION

When this research study was initiated, the Texas State Department of Highways and Public Transportation (TSDHPT) required the wood guardrail post to have a minimum diameter of 7 in. and a minimum soil embedment depth of 38 in. If the top of the post was domed, the minimum overall length was 69 in., and a minimum overall post length of 66 in. was required if the top of the post was beveled. The specifications stated that the steel W6 x 8.5 guardrail post should comply with the beveled wood post. When a guardrail is required at a culvert where the fill depth will not permit the full embedment depth of the guardrail post, a "rigid" bridge rail is now installed. This rigid bridge rail then calls for a special transition between the flexible guardrail.

The purpose of this research report was to determine the force vs. displacement characteristics and amount of energy absorbed by the lateral soil resistance produced on timber and steel standard guardrail posts embedded 18 in., 24 in., 30 in., and 38 in. in a cohensionless and cohesive soil. The post type, soil properties and length of embedment are important factors in determining the behavior of the guardrail system. This information will be used in other phases of this study to modify the guardrail design. Hopefully, more posts could be used with shallower embedment to achieve the desired strength.

This phase of the study consists of a series of static tests on timber and steel posts embedded 18 in., 24 in., 30 in. and 38 in. in two different types of soil. The work plan consisted of

1. An existing mathematical model for static laterally loaded guardrail posts was used to predict the lateral capacity of the post.
2. Soil tests were conducted to determine the average properties of the cohesive and cohensionless soils.
3. Static field load tests were performed on timber and steel posts with 18 in., 24 in., 30 in. and 38 in. with embedment depths in two types of soils.
4. The test results were compared with each other and with the mathematical model.

MATHEMATICAL MODEL

Using the fundamental earth pressure theory developed by Coulomb, the static post capacity could be estimated for each specific test condition using the model reported by Broms (1 and 2)*. For short, free ended, rigid piles in cohesive soils, the distribution of soil resistance along the pile was simulated by Broms (1) as shown in Fig. 1. The ultimate lateral soil pressure along the length is a function of the undrained shear strength, C_u, and the pile diameter B.

For cohesionless soils, Broms (2) uses the ultimate pressure distribution shown in Fig. 2. The ultimate soil pressure is defined in terms of γ, L, B and K_p; where γ is the effective unit weight of the soil, L is the embedment depth, B is the pile diameter and K_p is the Rankine passive earth pressure coefficient $K_p = \tan^2(45 + \phi/2)$.

The lateral capacity, P, for the cohesive and cohesionless soils can be determined by using moment and horizontal force static equilibrium equations. These lateral soil pressure distributions proposed by Broms are widely used in practice to predict the ultimate lateral capacity of a pile.

The ultimate lateral soil resistance for the cohensionless and cohesive soils was calculated using Broms' procedures at each embedment depth. These values are presented in Table 1. The lateral post capacity versus embedment depth are plotted in Figures 3 and 4. These static analysis results approximate the ultimate lateral soil capacity developed for each of the static load tests.

---

*Underscored numbers in parentheses correspond to numbers in the list of references.

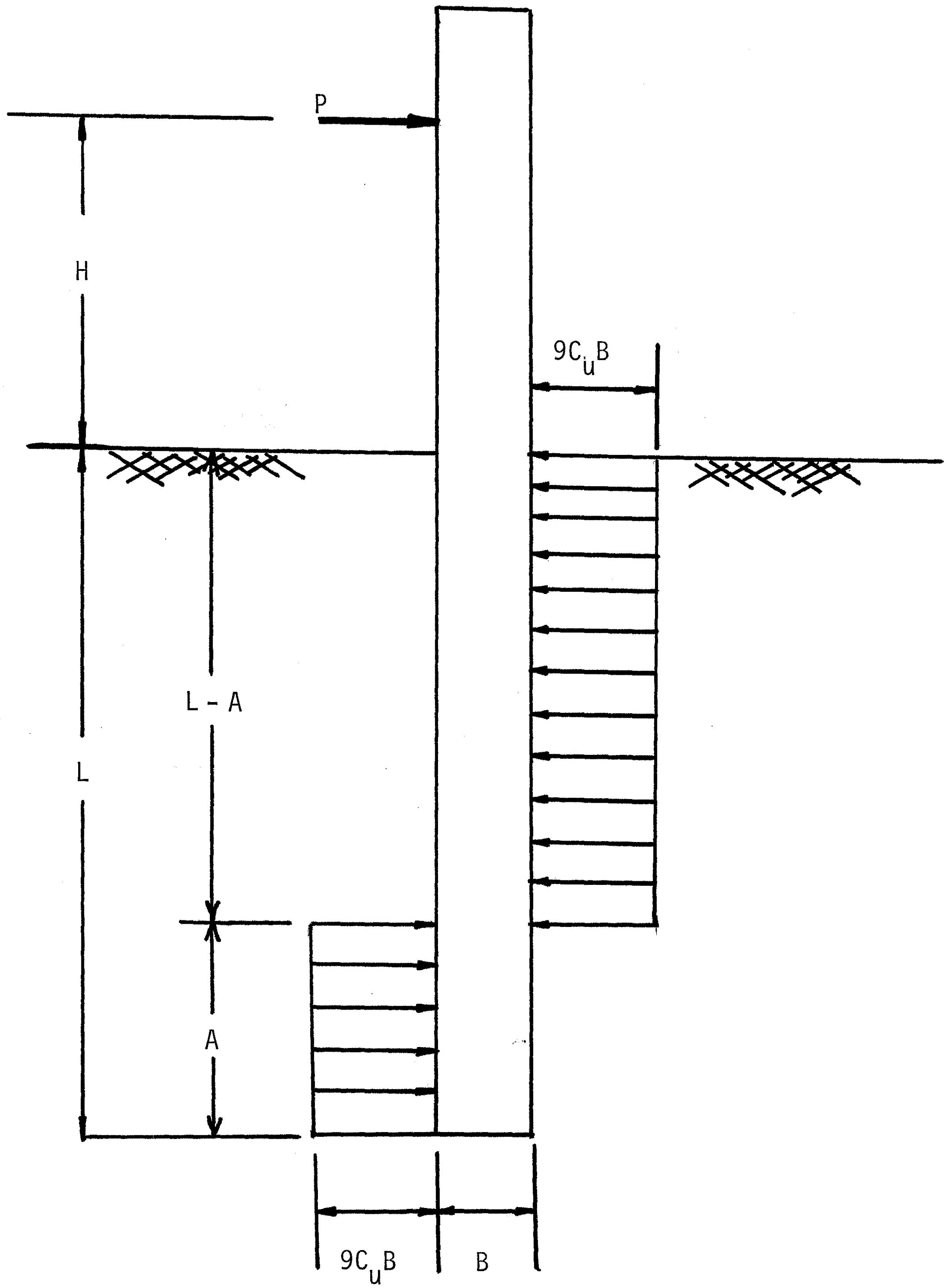

FIG. 1-Brom's Ultimate Lateral Soil Resistance for Cohesive Soils (Ref. 1)

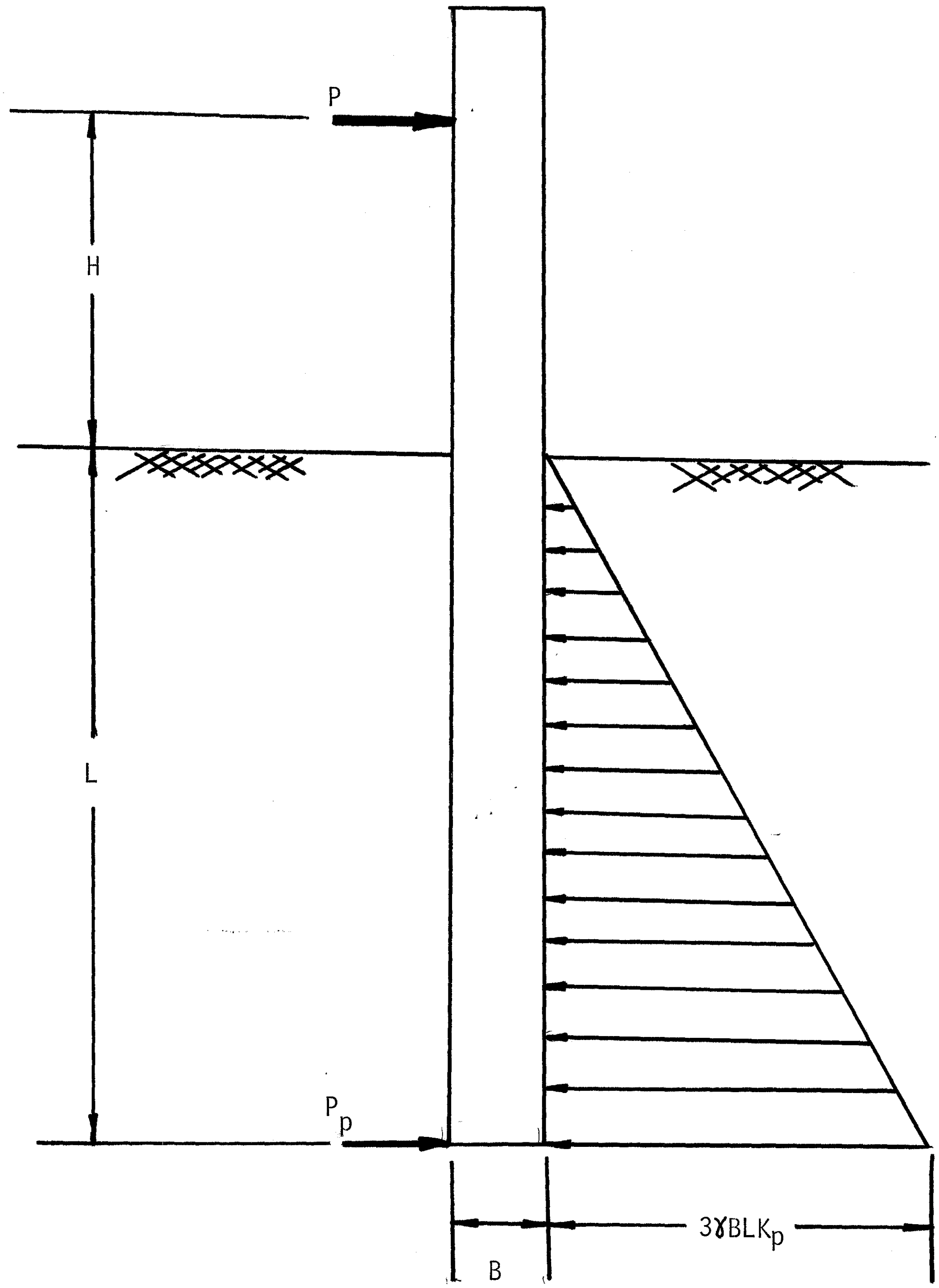

FIG. 2.-Brom's Ultimate Lateral Soil Resistance for Cohesionless Soils (Ref. 2)

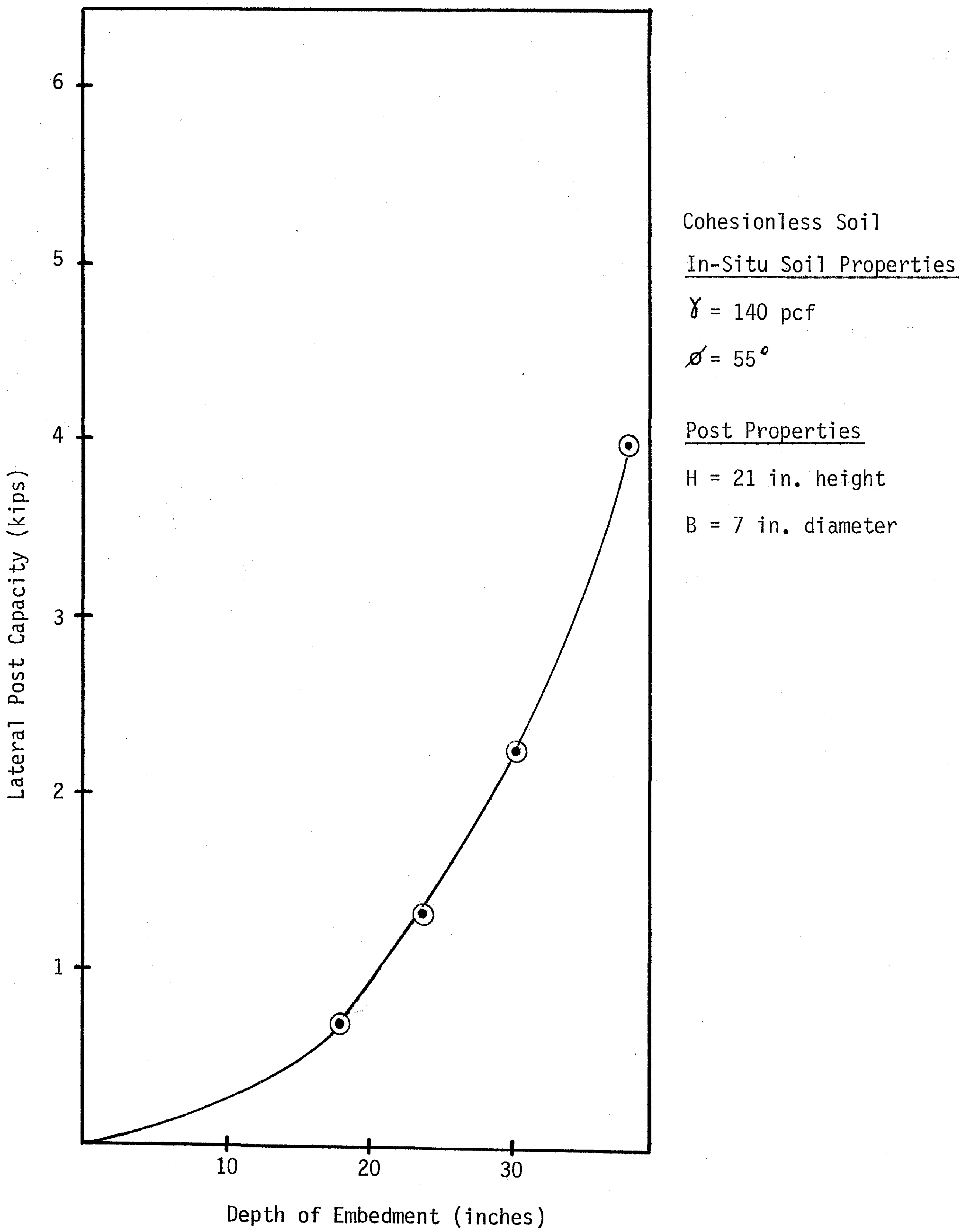

FIG. 3.-Lateral Load vs. Embedment Depth for Analytical Model (Cohesionless Soil)

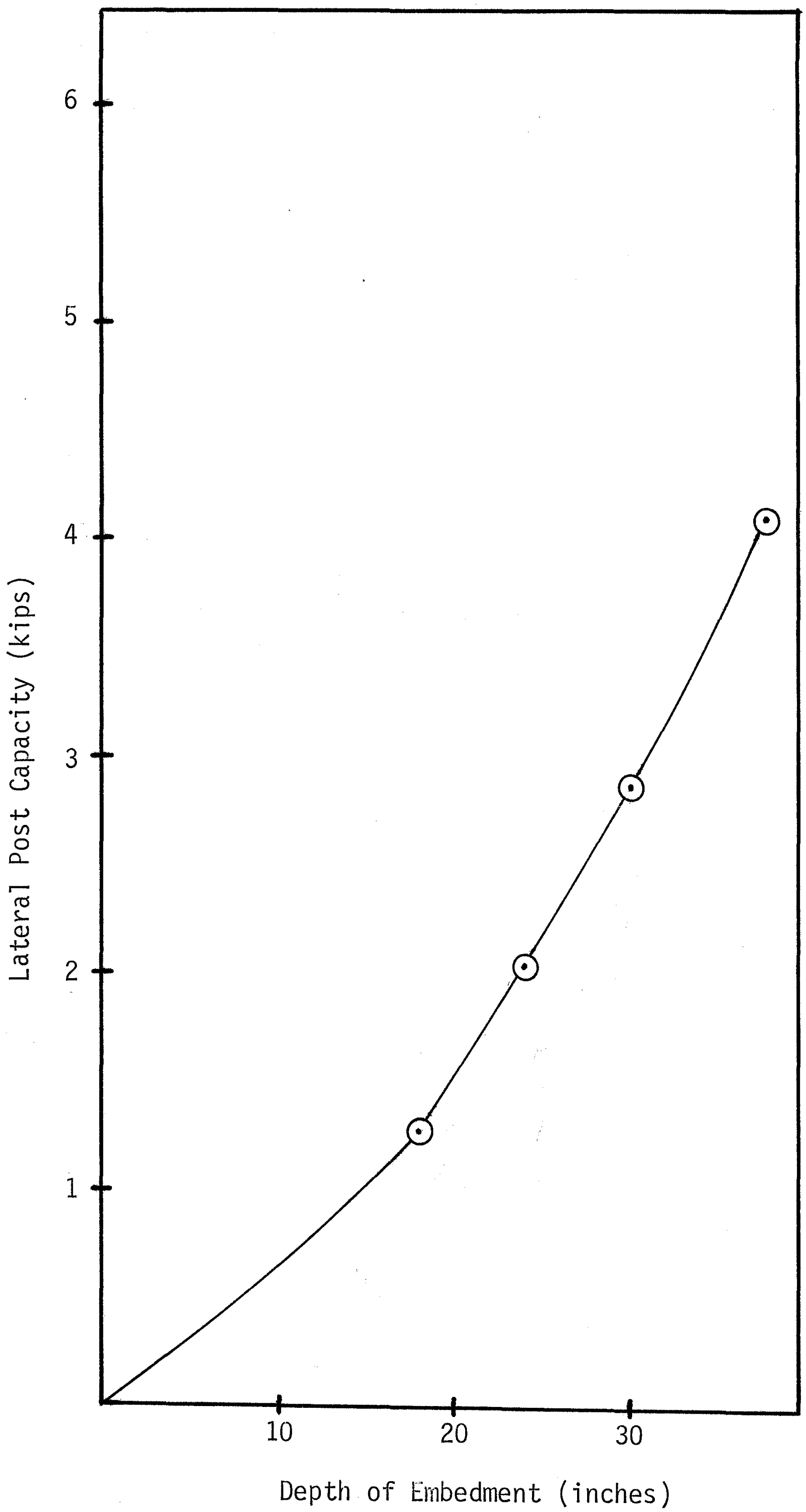

Cohesive Soil

In-Situ Soil Properties

σ = 15.5 psi

ϕ = 14.7°

$C_u = c + \sigma \tan\phi$

Post Properties

H = 21 in. height

B = 7 in. diameter

FIG. 4.-Lateral Load vs. Embedment Depth for Analytical Model (Cohesive Soil)

TABLE 1

SUMMARY OF STATIC ANALYSIS

<u>Cohesionless Soil</u>

γ = 140 pcf

$\phi = 55°$

<u>Post Properties</u>

Distance to Load = 21 in.

Post Diameter = 7 in.

Embedment Depth (inches)	Maximum Lateral Capacity, (kips)
18	0.7
24	1.3
30	2.3
38	4.0

<u>Cohesive Soil</u>

σ = 15.5 psi

$\phi = 14.7°$

c = 3.5 psi

$C_u = c + \sigma \tan\phi$

<u>Post Properties</u>

Distance to Load = 21 in.

Post Diameter = 7 in.

Embedment Depth (inches)	Maximum Lateral Capacity (kips)
18	1.3
24	2.0
30	2.9
38	4.1

SOIL CONDITIONS

To assess the effects of varying soil conditions, it was decided to perform a series of tests in two soils (cohensionless and cohesive) with different properties. The test site was located at the Texas A&M University Research and Extension Center. The test site is shown in Fig. 5. The natural soil at the test site was a stiff cohesive clay which was used as the cohesive soil. A pit had to be constructed to remove the cohesive soil and replace it with a selected cohensionless soil for those tests.

For the natural cohesive soil, two soil borings were used to determine the soil conditions at the test site. Undisturbed soil samples were taken with a 2.0 in. diameter thin-walled tube sampler. Laboratory tests on the samples included unit weights and moisture contents. A direct shear test was also conducted to determine the cohesive strength and angle of internal friction of the cohesive soil. The test results from these tests are shown in Table 2.

After the unconsolidated, undrained, direct shear tests were completed, a plot of shearing stress versus deflection was constructed as shown in Fig. 6. These curves were used to get the maximum shear strength of the soil for each normal stress to plot the strength envelope as shown in Fig. 7. The cohesion and angle of internal friction for the soil could be determined from Fig. 7. The test results indicated that the site consisted of a stiff clay.

The cohesionless soil used was a crushed limestone material obtained from near Georgetown, Texas. An existing stockpile containing this material was used. At the time the pit was constructed, the soil properties were determined using a McGuin water psychrometer and by taking soil samples for laboratory tests.

The in-situ unit weight was difficult to obtain from the McGuin water psychrometer test due to the large particle size of the soil. Conventional methods of shear strength determination could not be used because of the large particle size. To obtain the angle of shear resistance and cohesion, a sieve analysis and water content determination was conducted. A gradation curve, maximum particle size, relative density and overburden pressure were correlated to determine the shear strength and estimate the cohesion of the soil. The gradation curve obtained was constructed from the sieve analysis

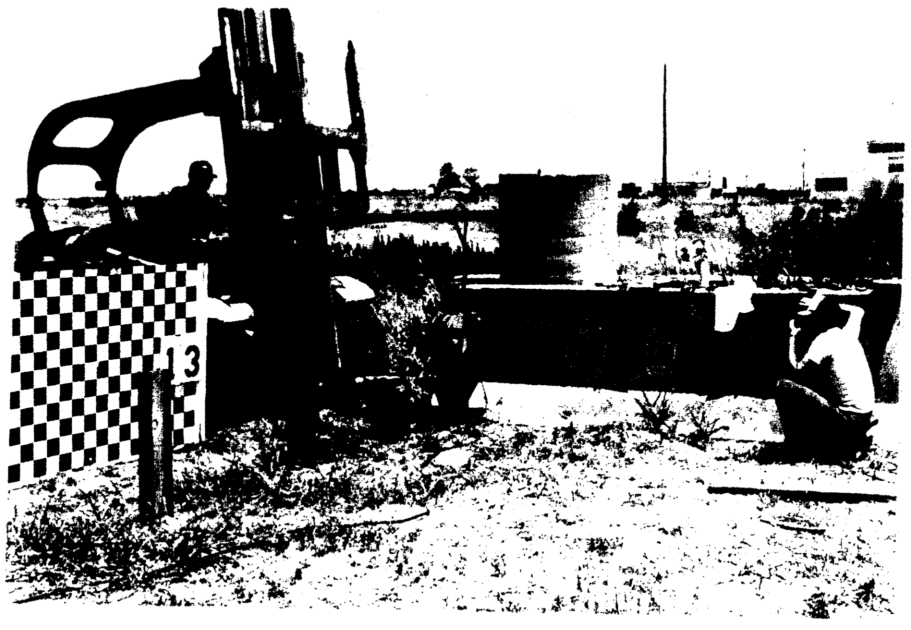

FIG. 5.-Test Site for Static Tests

Unconsolidated Undrained Direct Shear Test (UU)

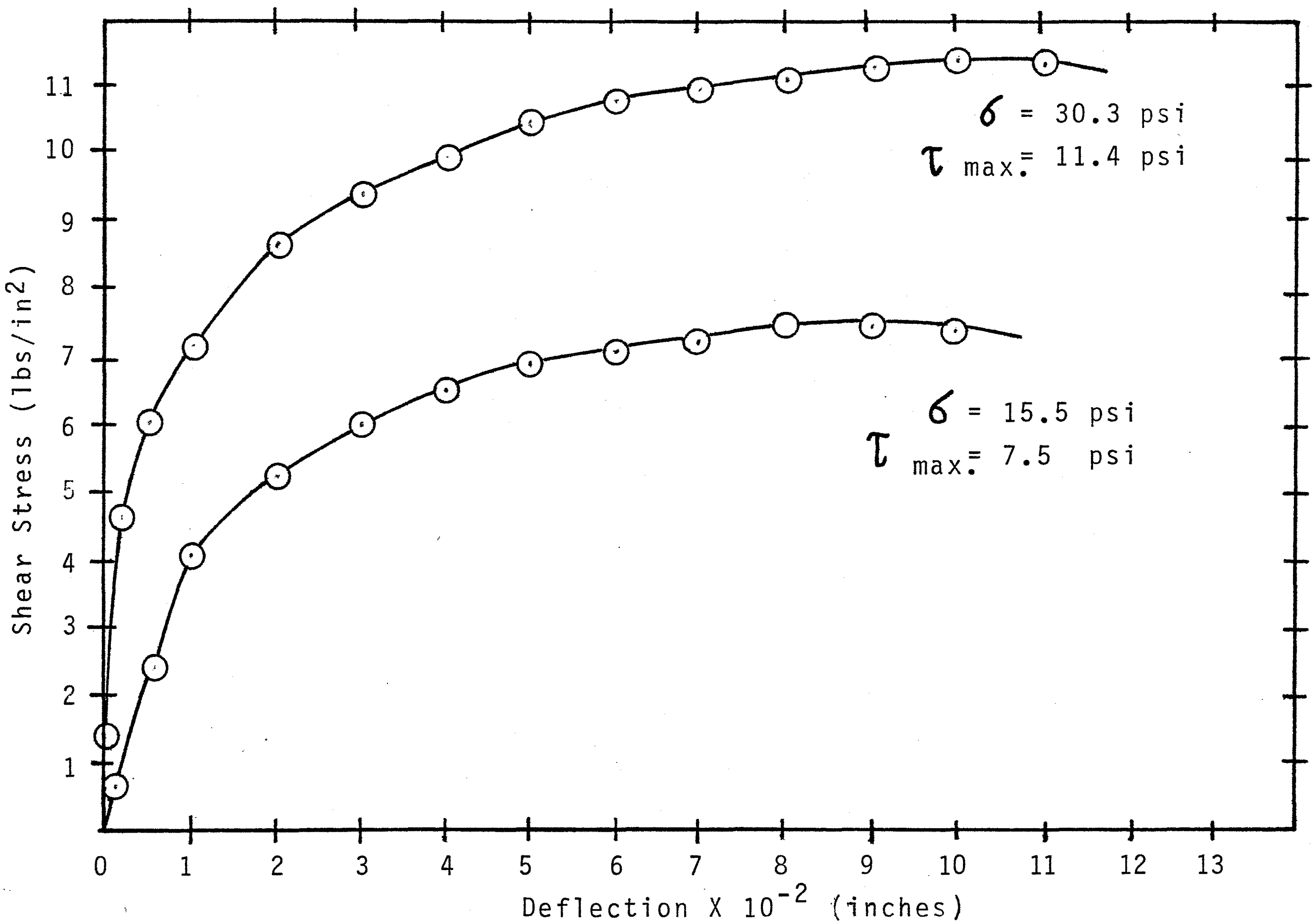

FIG. 6.-Shearing Stress vs. Deflection for Two Different Normal Stresses

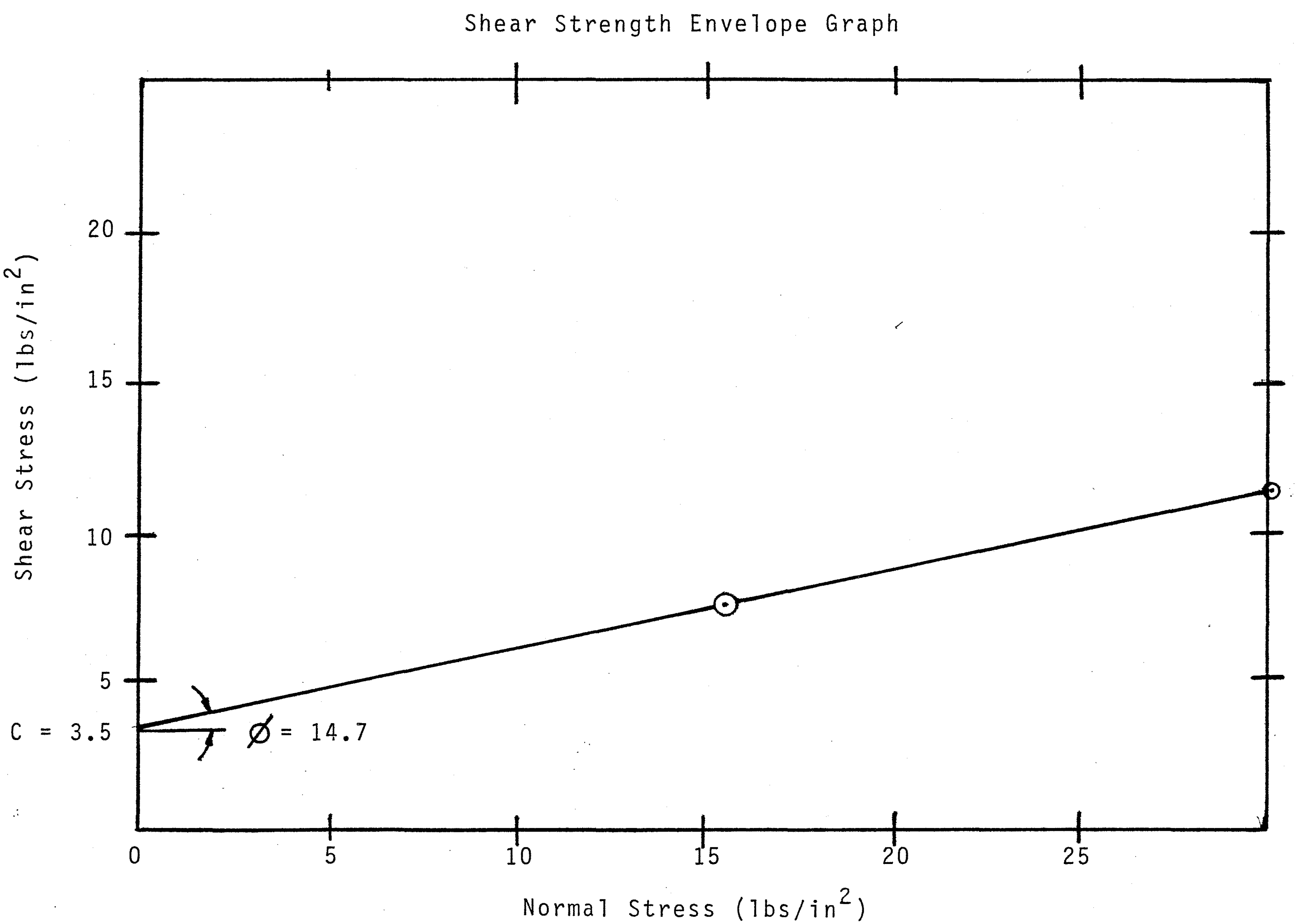

FIG. 7.-Shearing Stress vs. Normal Stress for Cohesive Soil

TABLE 2

PROPERTIES OF THE SOIL

	Cohesive Soil	Cohesionless soil
Generalized Description of the Soil	Dark, grey stiff clay	Well graded crushed limestone gravel
Total Unit Weight (γ_t), pcf	126.9	140
Average Moisture Content (w), %	21.8	——
Angle of Internal Friction (ϕ), °	14.7	48-55
Cohesion (C), psf	504	0-50

shown in Fig. 8. The gravel was classified as a GW (well graded gravel, gravel sand mixture, little or no fines) material of the Unified Soil Classification System. The large triaxial test results presented by Leps (3) are shown in Fig. 9. From these correlations a range of 48 to 55 degrees was chosen for the angle of internal friction. The gravel pit had a large variation of moisture content due to the entrapment of large pockets of water. The moisture content could not be determined because of this variation. The cohesion was estimated from the laboratory tests and engineering experience. The properties of the cohensionless soil are also summarized in Table 2.

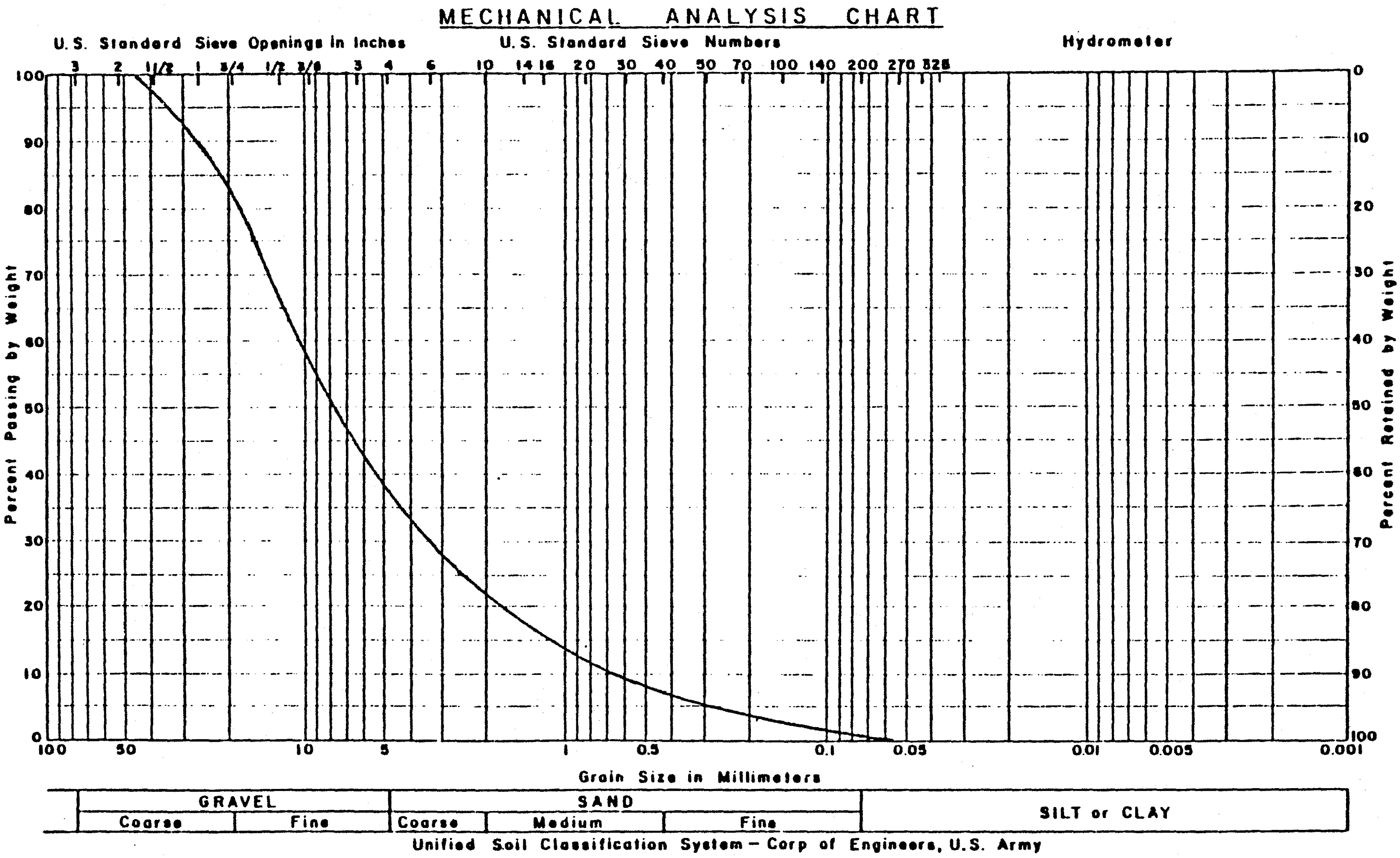

FIG. 8. -Gradation Curve for the Cohesionless Soil

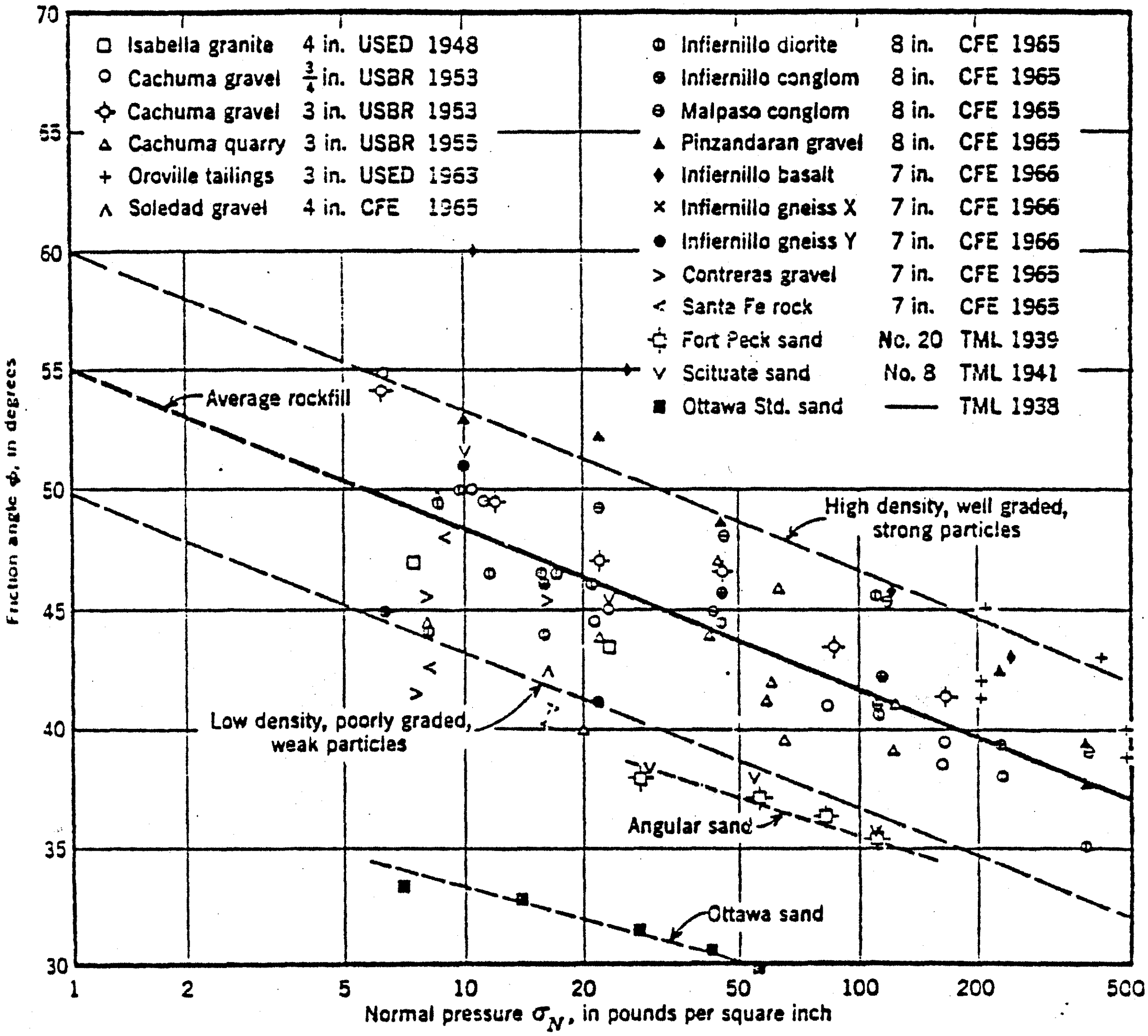

FIG. 9. -Shear Strength of Rockfill Materials from Large Triaxial Tests (after Leps (3))

STATIC LOAD TESTS

INTRODUCTION

A series of static guardrail post tests were conducted to determine the effects of embedment depth, soil conditions and post type on the load deformation characteristics of the posts. The effects of reducing the embedment could be determined from the comparison of energy absorbed by the soil-post system. It would be much more economical to have a guardrail system with a few posts embedded 18 in. that would enable a culvert to extend beneath. Currently, the TSDHPT requires a rigid bridge rail when full embedment depth cannot be achieved. These types of traffic rail systems are expensive to construct and sometimes cause a transition problem between the flexible guardrail system and the rigid bridge rail system.

TESTING PROGRAM

The static guardrail tests that were conducted are summarized in Table 3. A total of 16 tests was performed, eight in cohesive soil and eight in cohensionless soil. Both steel and timber posts were used with embedment depths of 18 in., 24 in., 30 in. and 38 in. for the comparison of energy absorption.

PLACEMENT OF POST

The test setup and location of the posts are shown in Figs. 10 through 13. To assess the effects of varying soil conditions, the posts were placed in two soils with significantly different properties. A cohensionless gravel and a stiff cohesive clay were used for this purpose.

The posts were placed in the soil by augering a 24 in. diameter hole and tamping the soil around the post in several lifts. After the posts were tamped in place, a four-to-five week period followed to allow the soil to consolidate, relieve construction stresses and to become more uniform with the surrounding soil conditions.

EQUIPMENT AND INSTRUMENTATION

In order to conduct the tests, a loading system had to be constructed capable of (1) applying a horizontal force to the post at a uniform

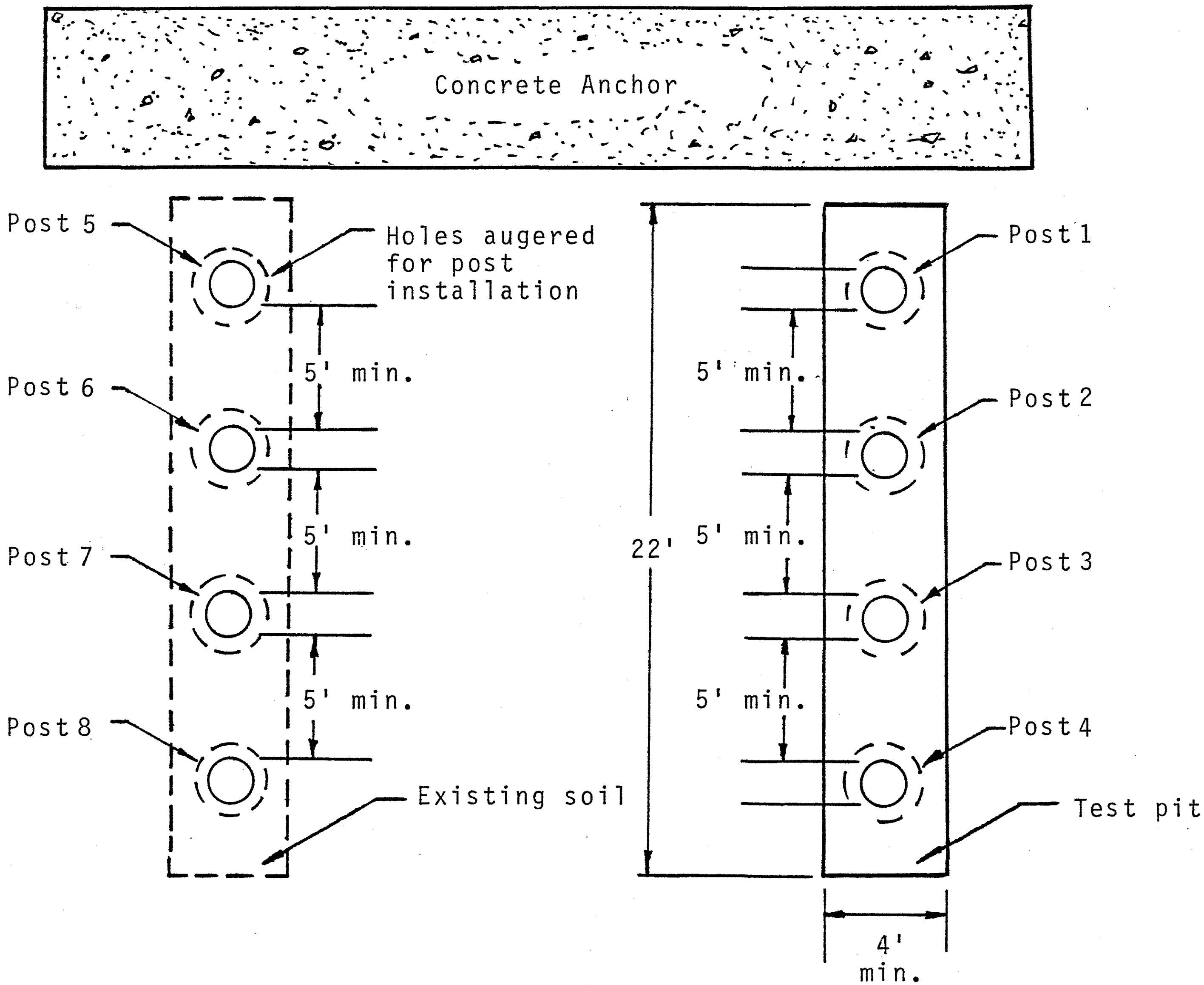

FIG. 10-Location of Posts 1-8

Placement of timber posts

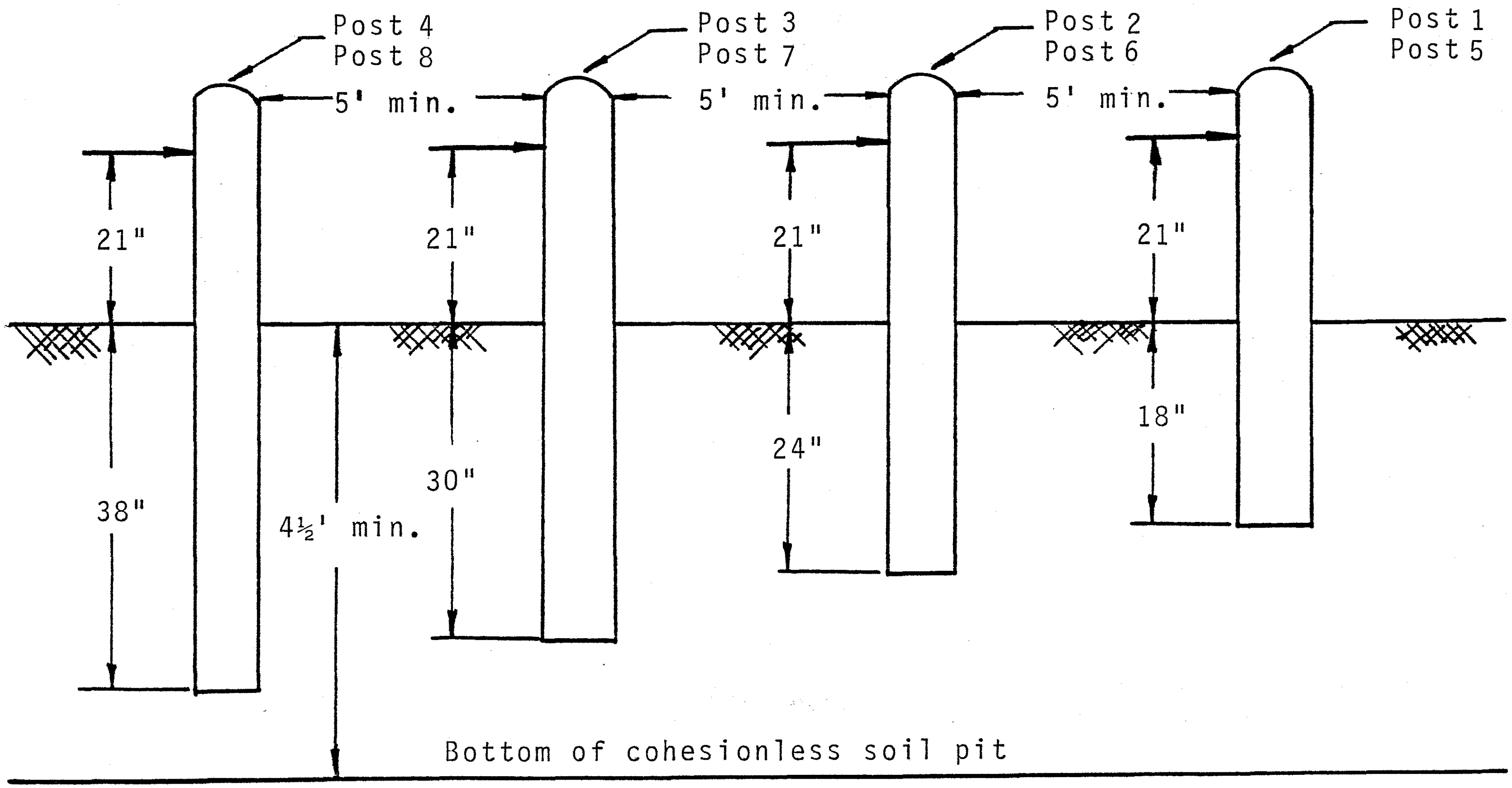

FIG. 11.-Placement of Timber Posts 1-8

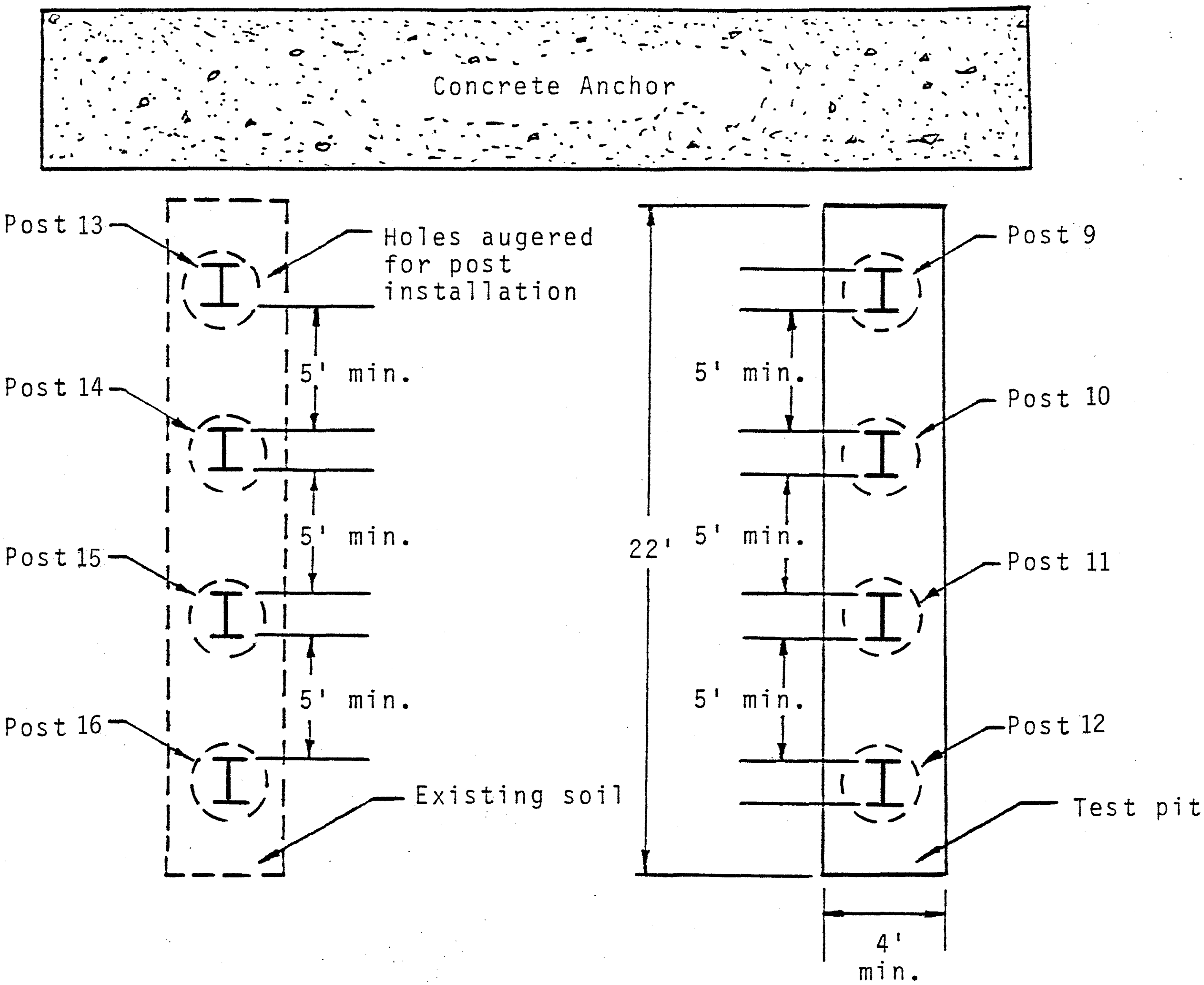

FIG. 12.-Location of Steel Posts 9-16

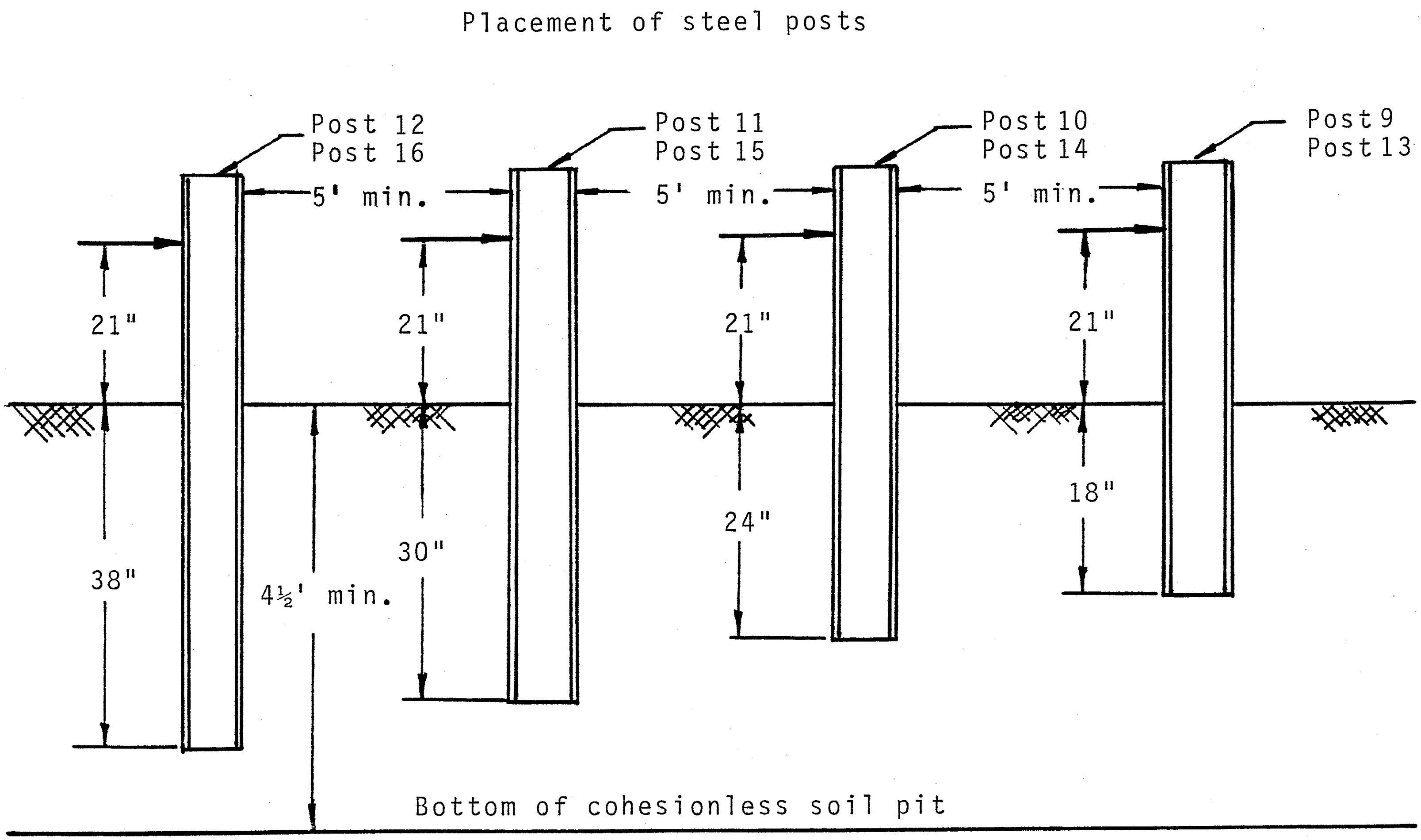

FIG. 13-Placement of Steel Posts 9-16

TABLE 3

SUMMARY OF TESTS

Test No.	Post Type	Embedment Depth (in.)	Height of Load (in.)	Soil Type
1	Wood	18	21	Cohesionless
2	Wood	24	21	Cohesionless
3	Wood	30	21	Cohesionless
4	Wood	38	21	Cohesionless
5	Wood	18	21	Cohesive
6	Wood	24	21	Cohesive
7	Wood	30	21	Cohesive
8	Wood	38	21	Cohesive
9	Steel	18	21	Cohesionless
10	Steel	24	21	Cohesionless
11	Steel	30	21	Cohesionless
12	Steel	38	21	Cohesionless
13	Steel	18	21	Cohesive
14	Steel	24	21	Cohesive
15	Steel	30	21	Cohesive
16	Steel	38	21	Cohesive

displacement rate, (2) measuring the load acting on the post and (3) measuring the displacement of the post at ground level and at a height of 21 in. To apply the lateral force, a pulley was mounted to a concrete anchor at a height of 21 in. above ground level. A cable was placed through the pulley and attached to the load cell. The free end was attached to a fork lift truck. The fork lift truck slowly raised the cable upward, applying the lateral load to the post. This loading system is shown in Fig. 14.

The load applied to the post was measured by a load cell force transducer attached to the loading bracket as shown in Fig. 15. Before the test, the transducer was calibrated up to a maximum load of 15 kips. The force transducer was constructed of a metal bar instrumented with a full bridge of strain gages. The output from these strain gages was measured with a digital microvoltmeter calibrated to read the load directly. For the series of static tests 1 through 4, the post deflections at the ground surface were measured. In order to locate the pivot point of the post, a second measurement was taken close to the top of the post. For energy absorption comparison, the measured horizontal deflections were graphically converted to deflections at a height of 21 in. For the series of tests 5 through 16 the horizontal deflections were measured once at a height of 21 in. The post displacements were measured with a measuring tape from a fixed point about 5 ft behind the post.

TEST PROCEDURE

A specially constructed loading bracket was attached to the post at a height of 21 in. above the ground. The brackets for the steel and timber posts are shown in Figs. 16 and 17. The bracket allowed a horizontal pull throughout the displacement of the post and eliminated the development of stress concentrations in the post. The load transducer was attached to the loading bracket and cable. A small amount of tension was transferred to the cable by raising the forks of the lift truck to take out the initial slack in the loading system. After the calibration number was checked, the load transducer was zeroed. The load was read off the digital microvoltmeter at every one-half inch of movement of the post. The test continued until the post began pulling out of the ground.

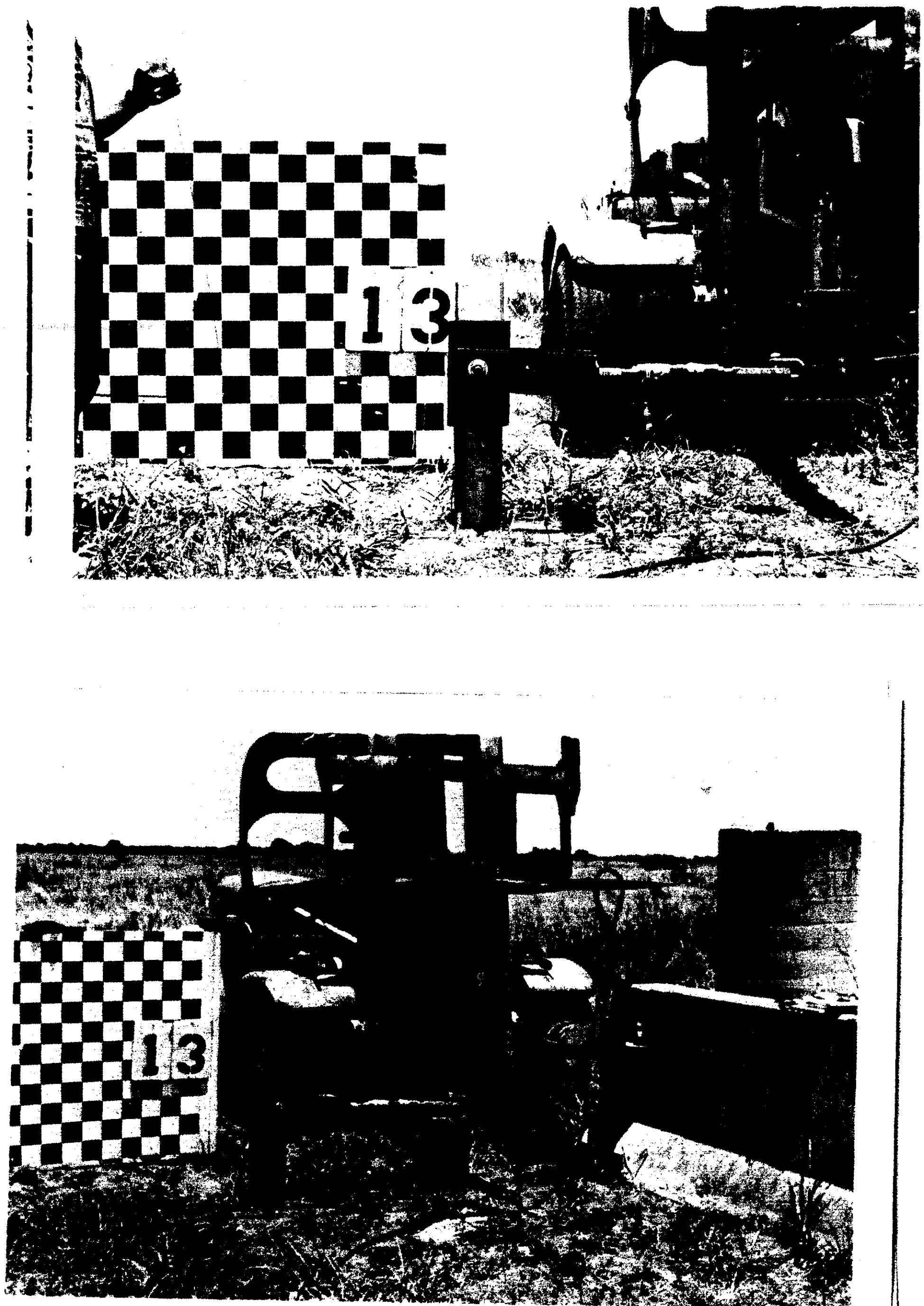

FIG. 14.-Static Testing System

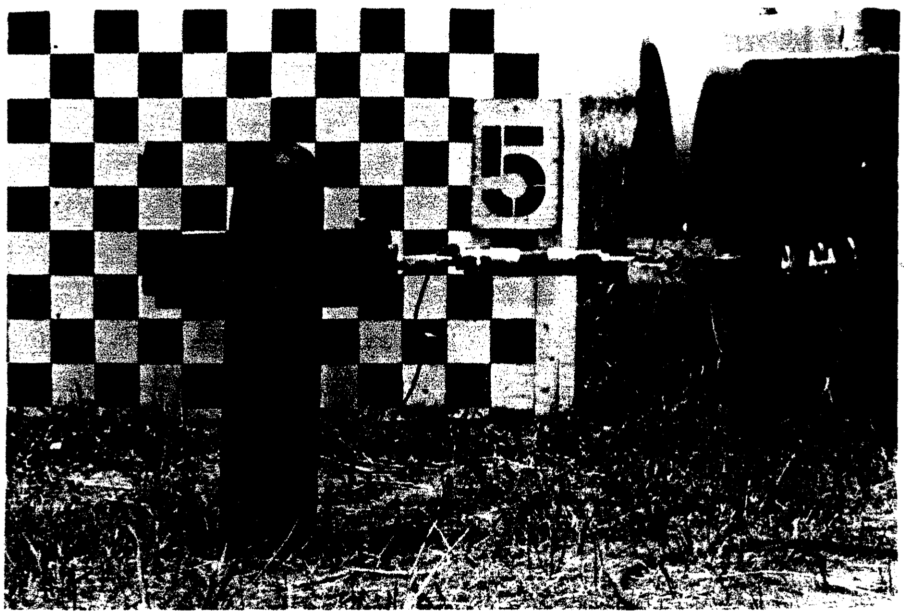

FIG. 15.-Attachment of Force Transducer to the Loading Bracket

FIG. 16-Loading Bracket for Timber Post

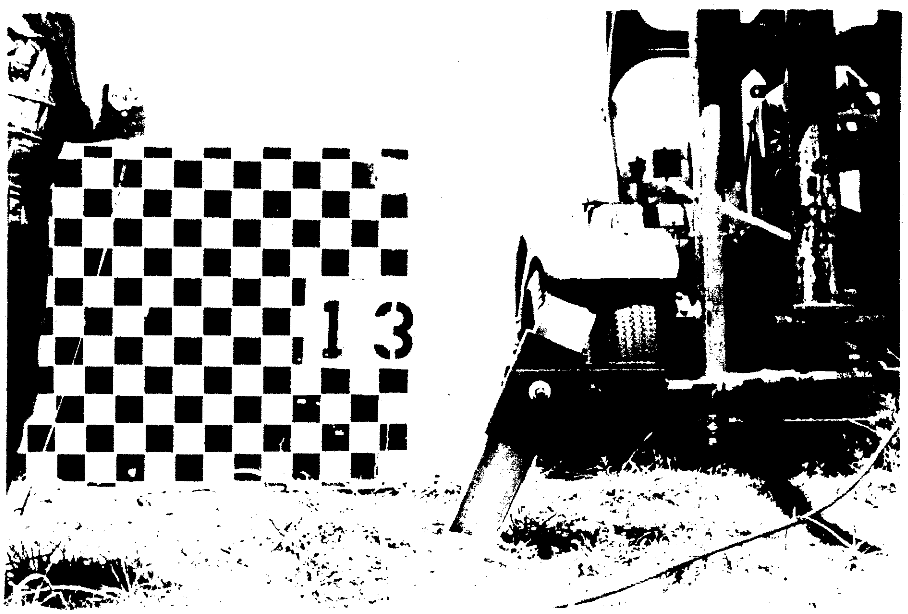

FIG. 17.-Loading Bracket for Steel Post

RESULTS AND CONCLUSIONS

STATIC TEST RESULTS

The lateral load versus deflection curves for the timber and steel posts are summarized in Figs. 18 to 21. Maximum lateral load values and dissipated energy are presented in Table 4.

For most cases the steel post proved to have a slightly smaller ultimate load and less energy absorption than the timber post with corresponding embedment depths and soil conditions. This was true for all tests except for the steel post embedded 38 in. in cohesive soil. The cohesive soil dissipated more energy than the cohesionless soil for the posts embedded 18 and 24 in. For posts embedded 30 and 38 in., the cohesionless soil absorbed more energy. A significant amount of energy absorbed by the soil was lost by reducing the embedment depth of the guardrail post. The percent differences of the absorbed energy and ultimate lateral capacity between the standard 38 in. embedded post and the other post with similar soil conditions are shown in Table 5. Tables 6 and 7 are provided from TTI Research Report 343-1 (4) and 343-1 Supplement (5) for additional comparisons.

COMPARISON OF TEST RESULTS WITH THEORETICAL PREDICTIONS

The lateral post capacity versus embedment depth for each static test are plotted with the analytical predictions in Figs. 22 and 23. The actual field test parameters used in calculating the theoretical curve were summarized previously in Table 1. For the cohensionless soil, the theoretical curve underpredicts the actual lateral capacity of the post. This could have been caused by the variation of the soil properties after the soil test samples were taken. The analytical model is also sensitive to the angle of internal friction. This parameter could only be estimated because of inconsistency of the cohesionless soil conditions. The predicted lateral loads for the cohesive soils closely followed the field load test results.

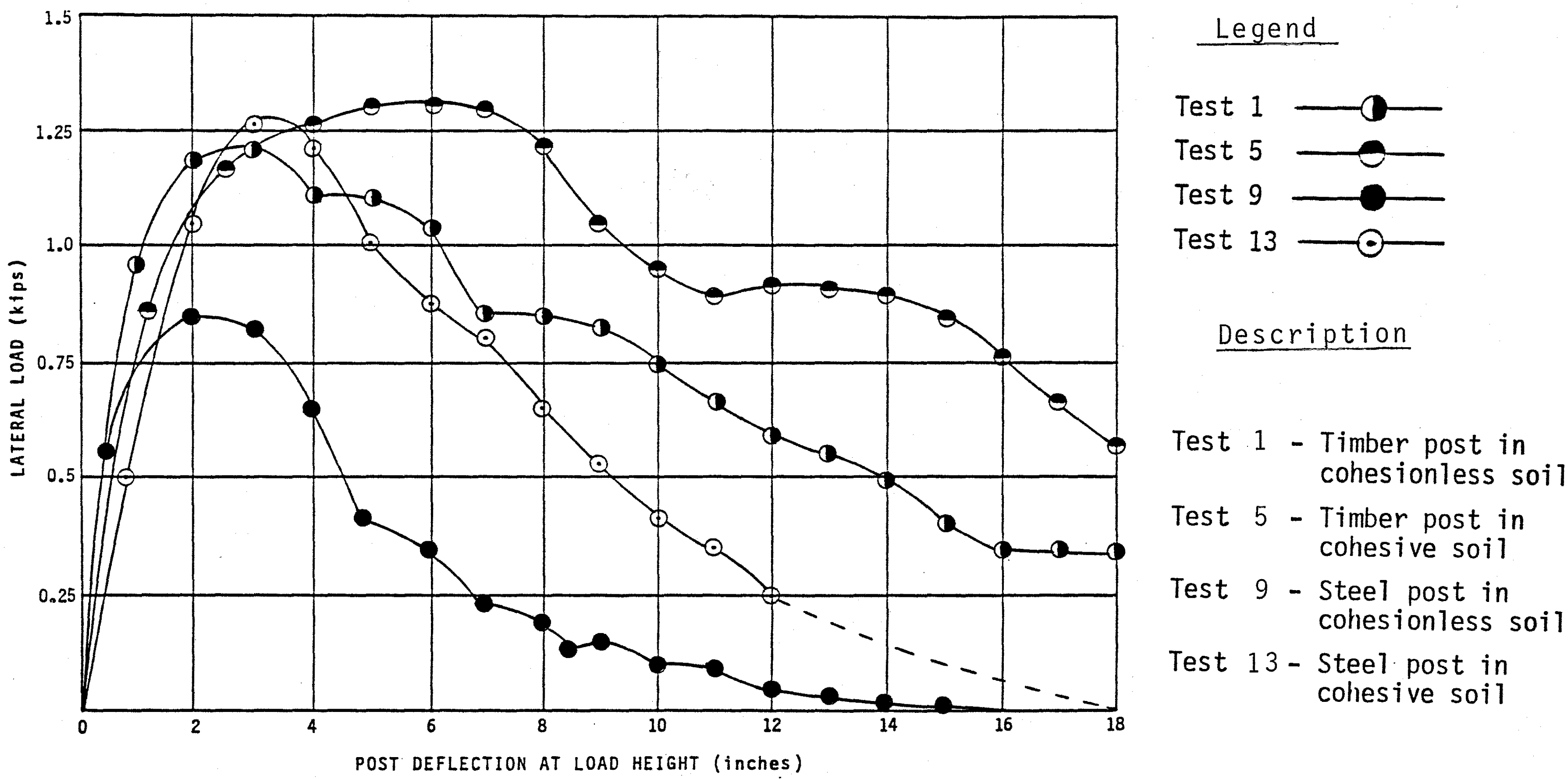

FIG. 18.-Lateral Load vs. Deflection for Post Embedded 18 in.

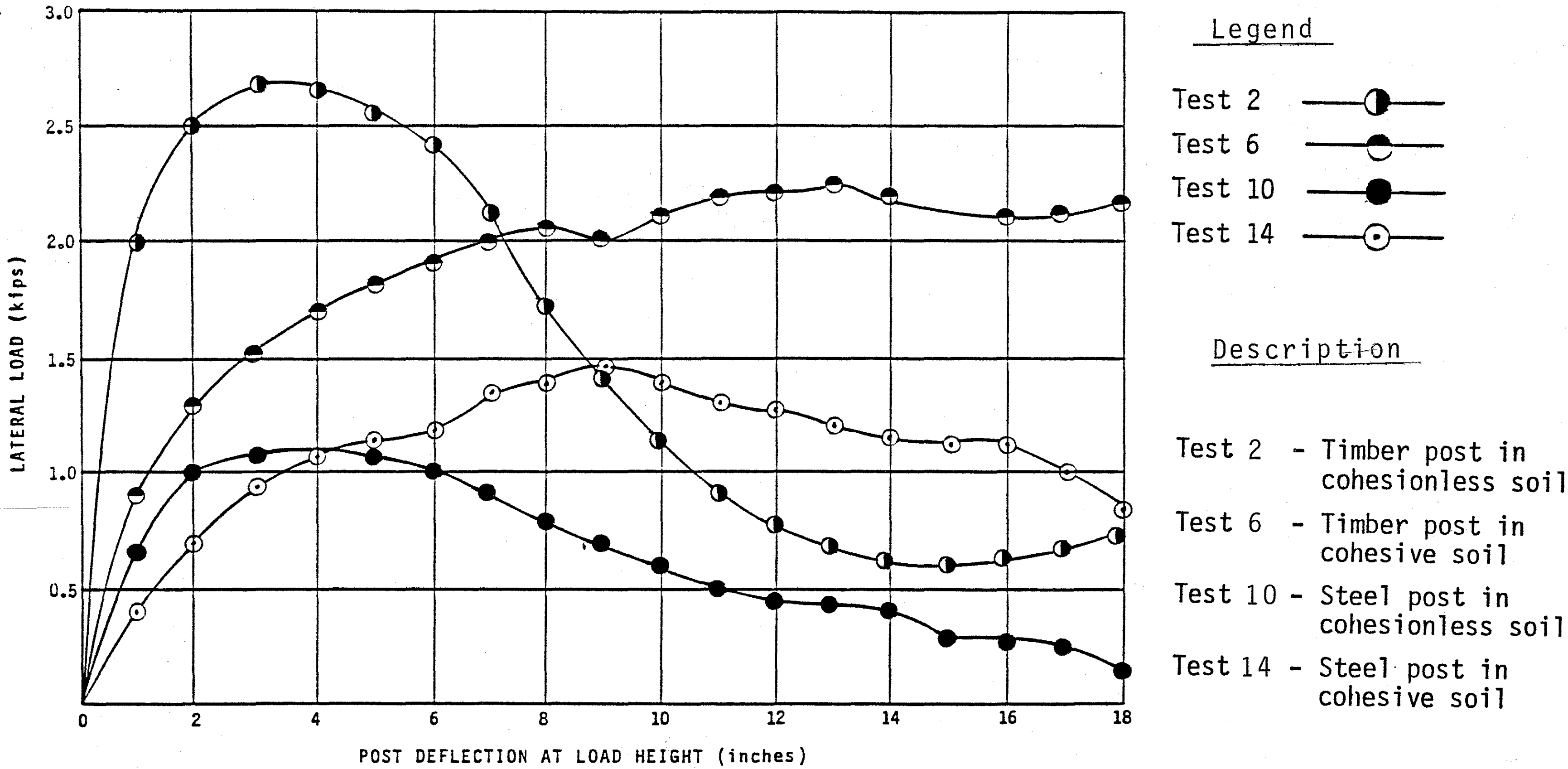

FIG. 19.-Lateral Load vs. Deflection for Post Embedded 24 in.

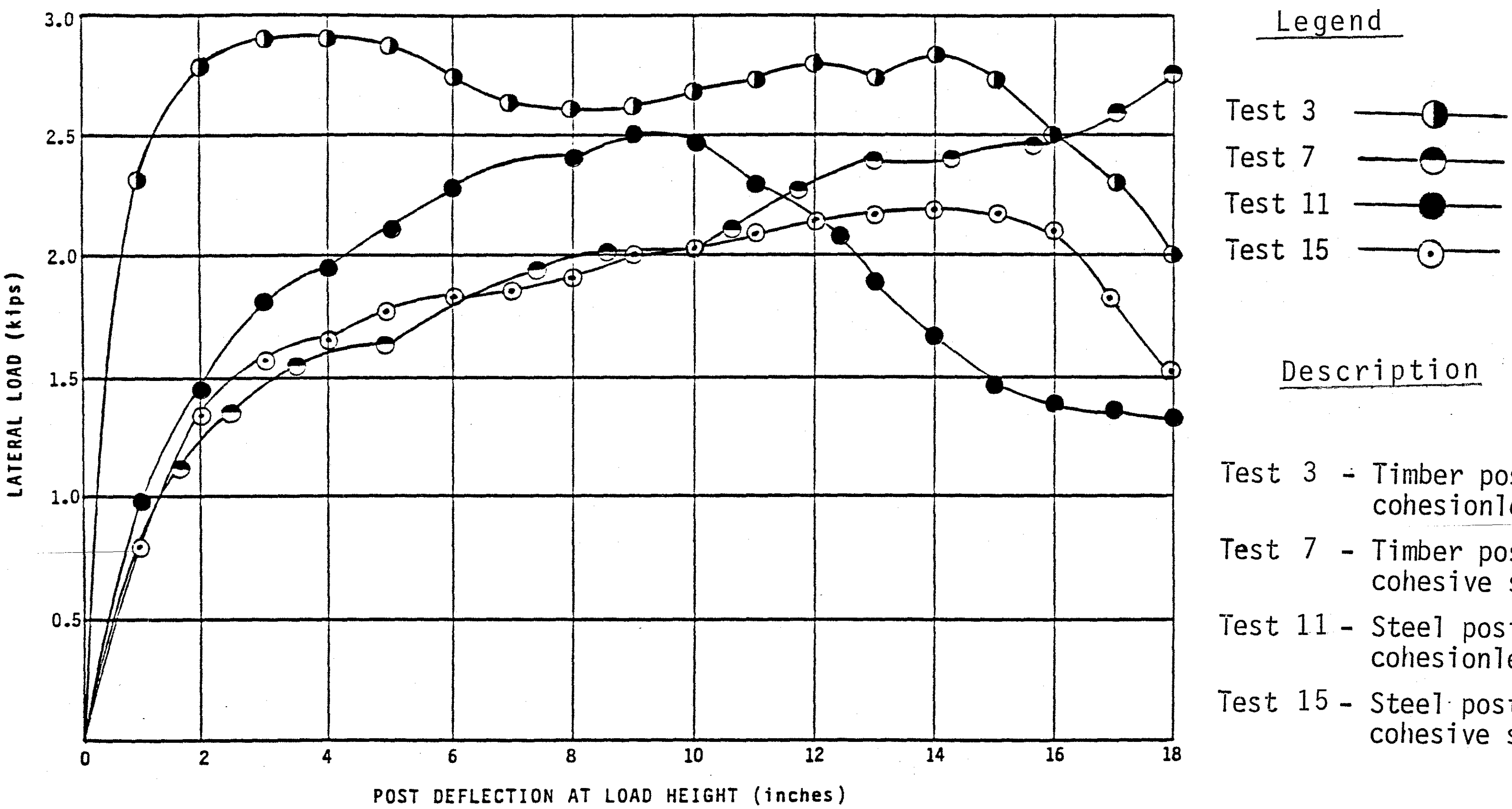

Description

Test 3 - Timber post in cohesionless soil

Test 7 - Timber post in cohesive soil

Test 11 - Steel post in cohesionless soil

Test 15 - Steel post in cohesive soil

FIG. 20.-Lateral Load vs. Deflection for Post Embedded 30 in.

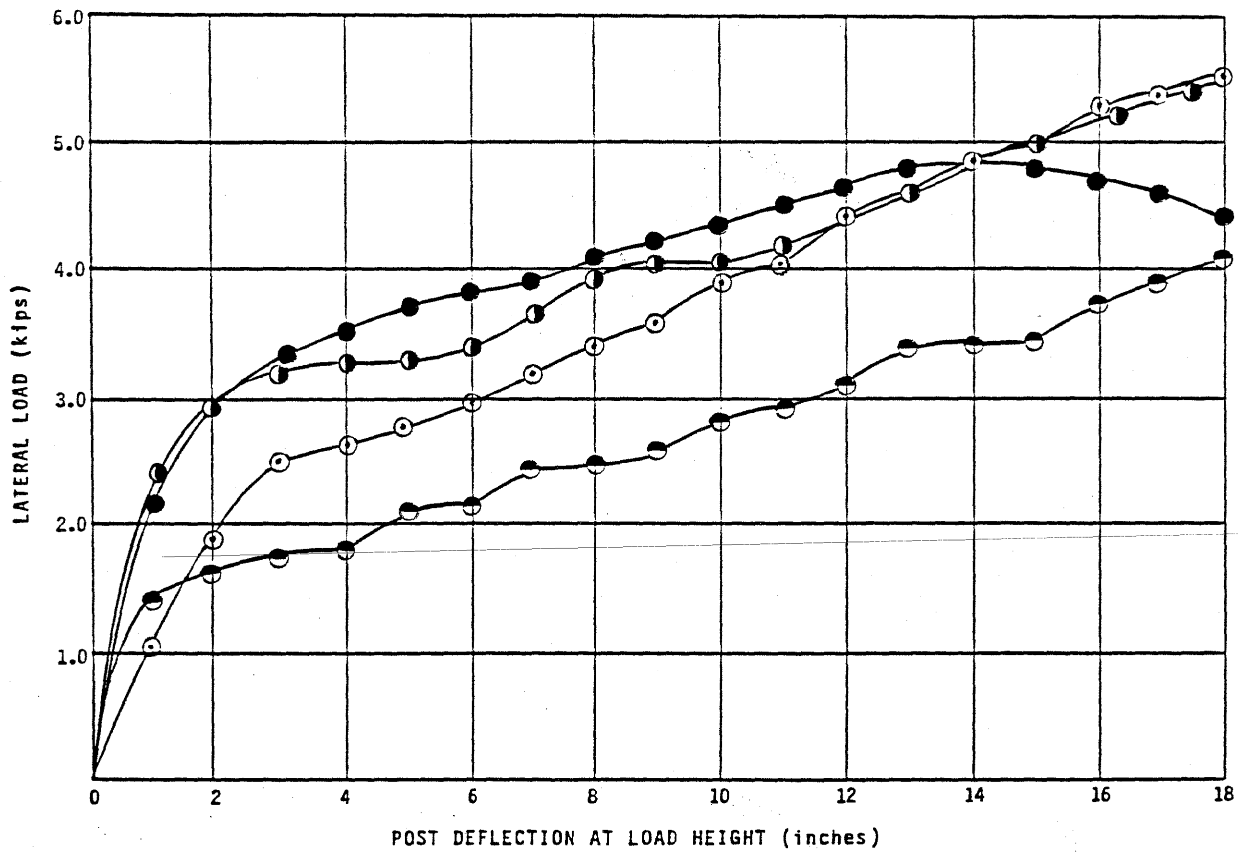

Legend

Test 4
Test 8
Test 12
Test 16

Description

Test 4 - Timber post in cohesionless soil

Test 8 - Timber post in cohesive soil

Test 12 - Steel post in cohesionless soil

Test 16 - Steel post in cohesive soil

FIG. 21.-Lateral Load vs. Deflection for Post Embedded 38 in.

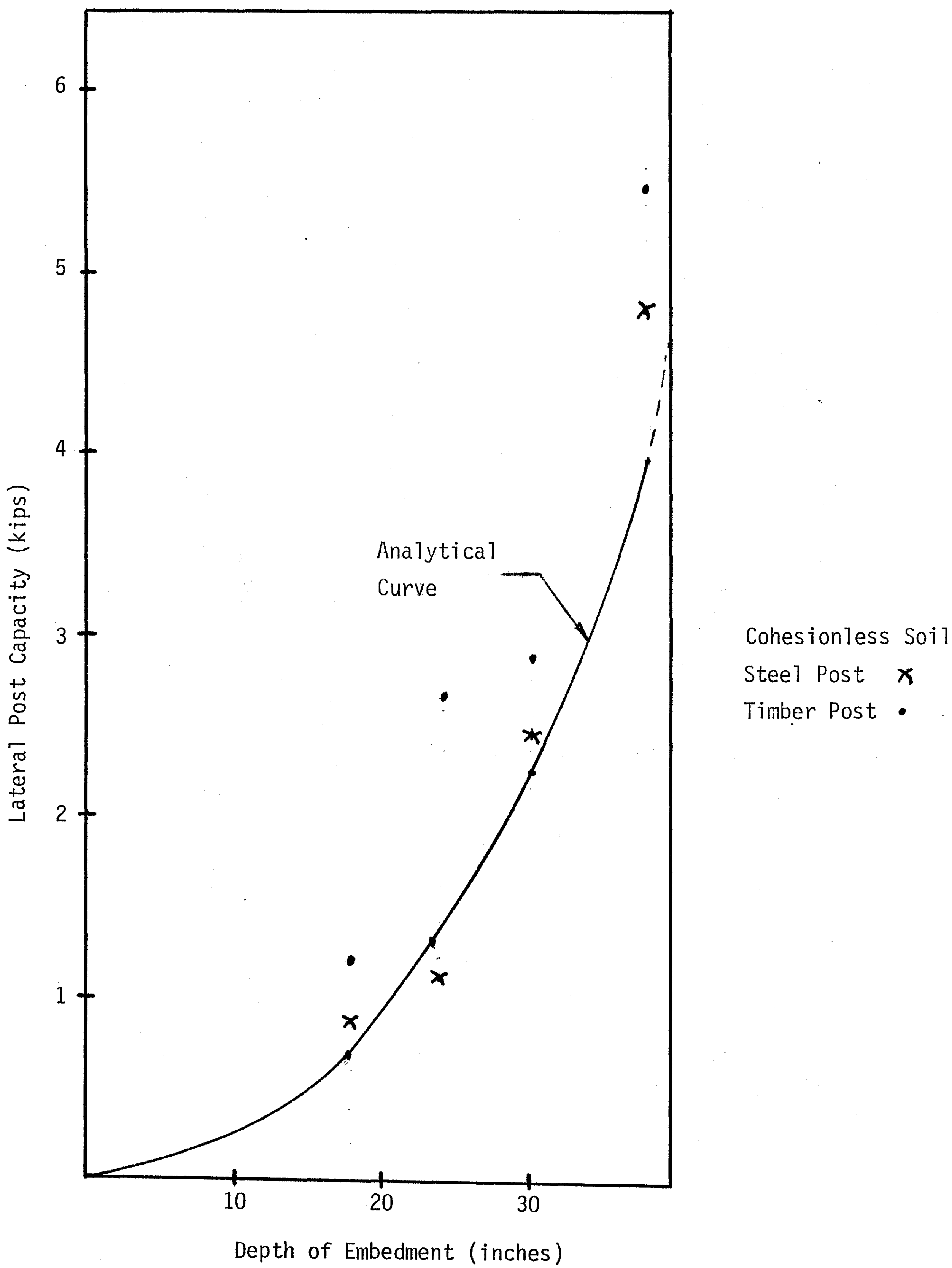

FIG. 22.- Comparison of Analysis and Field Load Tests 1-4 and 9-12

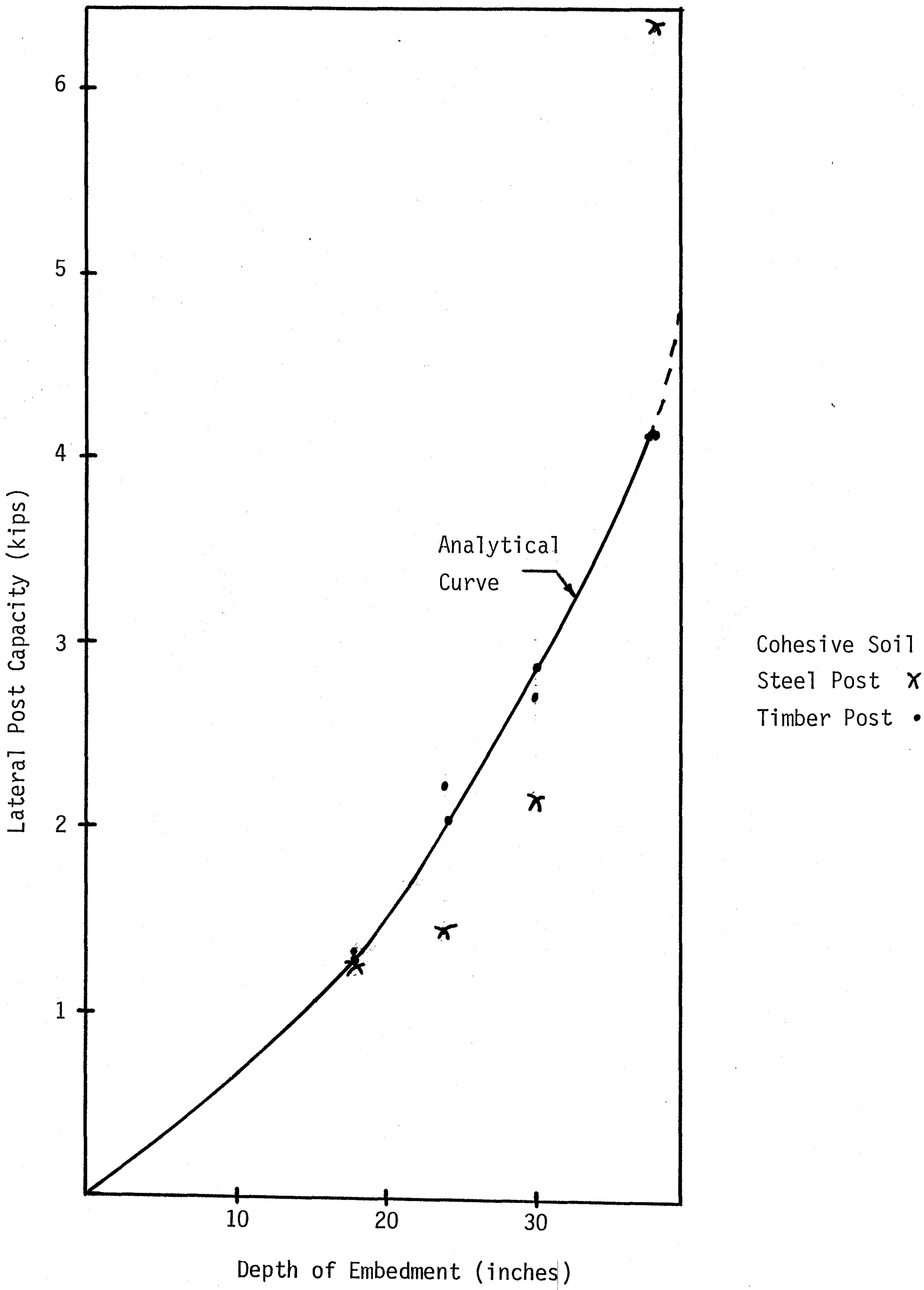

FIG. 23. -Comparison of Analysis and Field Load Tests5-8 and 13-16

TABLE 4

SUMMARY OF RESULTS

Test No.	Post Type	Soil Type	Maximum * Force (kips)	Energy** (kips-ft)
1	Wood	Cohesionless	1.20	1.1
2	Wood	Cohesionless	2.71	2.2
3	Wood	Cohesionless	2.92	4.0
4	Wood	Cohesionless	5.47	6.0
5	Wood	Cohesive	1.32	1.5
6	Wood	Cohesive	2.24	2.8
7	Wood	Cohesive	2.74	3.0
8	Wood	Cohesive	4.08	4.0
9	Steel	Cohesionless	0.86	0.4
10	Steel	Cohesionless	1.10	1.0
11	Steel	Cohesionless	2.51	2.8
12	Steel	Cohesionless	4.81	6.0
13	Steel	Cohesive	1.28	0.8
14	Steel	Cohesive	1.46	1.7
15	Steel	Cohesive	2.17	2.7
16	Steel	Cohesive	5.54	5.5

*Maximum force reached through 18 inches of horizontal deflection.
**Energy dissipated after 18 inches of horizontal deflection.

TABLE 5

PERCENT OF STATIC POST TEST WITH AN EMBEDMENT DEPTH OF 38 INCHES

TEST NO.	POST TYPE	SOIL TYPE	PERCENT OF MAXIMUM FORCE	PERCENT OF ENERGY
1	Timber	Cohesionless	21.9	18.3
2	Timber	Cohesionless	49.5	36.7
3	Timber	Cohesionless	53.4	66.7
The values above are percentages of test 4..				
5	Timber	Cohesive	32.4	37.5
6	Timber	Cohesive	54.9	70.0
7	Timber	Cohesive	67.2	75.0
The values above are percentages of test 8.				
9	Steel	Cohesionless	17.9	6.7
10	Steel	Cohesionless	22.9	16.7
11	Steel	Cohesionless	52.2	46.7
The values above are percentages of test 12.				
13	Steel	Cohesive	23.1	14.5
14	Steel	Cohesive	26.4	30.9
15	Steel	Cohesive	39.2	49.1
The values above are percentages of test 16.				

TABLE 6 - COMPARISON OF WOOD AND STEEL GUARDRAIL POSTS IN COHESIVE AND COHESIONLESS SOIL - STATIC AND IMPACT TESTS (Ref. 4)

TEST NO.	TYPE POST	TYPE SOIL	STATIC TEST		IMPACT TEST 17 MPH	
			MAX. LOAD KIPS	MAX. ENERGY* KIP-FT	MAX. LOAD KIPS	MAX. ENERGY* KIP-FT
1	WOOD	COHESIVE	3.7	4.2	16.3	19.2
2	STEEL	COHESIVE	3.3	3.8	17.0	17.1
	WOOD	COHESIONLESS	3.2	4.4 ✓	13.3	POST BROKE
	STEEL	COHESIONLESS	3.3	4.2	22.4	22.4

EMBEDMENT DEPTH - 38 IN., LOAD HEIGHT - 21 IN.

COHESIVE SOIL = 124 PCF C = 2 KSF

COHESIONLESS SOIL = 119 PCF $\phi = 50^{\circ}$

*MAX. POST DEFL. WAS 18 IN.

TABLE 7 - STRENGTH OF TIMBER GUARDRAIL POSTS
IN ROCK - 12 IN. DIAM. HOLE 18 IN. DEEP
HOLE BACKFILLED WITH CONCRETE, SAND, LIMESTONE, CLAY (Ref. 5)

TEST NO.	TYPE POST	TYPE SOIL	STATIC TEST MAX. LOAD KIPS	STATIC TEST MAX. ENERGY KIP-FT
1B	WOOD	ROCK-CONC.	9.9	2.7
2B	WOOD	ROCK-SAND	8.5	3.5
3B	WOOD	ROCK-LIMES.	8.4	3.2
4B	WOOD	ROCK-CLAY	11.4	4.2
			MAX. DEFL. 3 TO 8 IN.	MAX. DEFL. 10 TO 14 IN.

CONCLUSIONS

The conclusions that can be drawn from this research study are as follows:

1. The analytical model can be used for the analysis of laterally loaded guardrail posts. The comparison of the test results with the analytical predictions indicate that the analysis procedures are fairly reliable for short, free-ended, statically loaded piles (posts).
2. The static guardrail post tests conducted indicate that the steel posts tend to absorb less energy than timber posts. The cohesive soil dissipates more energy than cohesionless soil for posts embedded 18 and 24 in. For posts embedded 30 and 38 in., the cohesionless soil absorbs more energy. The amount of energy absorbed by the soil is significantly reduced by decreasing the embedment depth of the post.
3. It should be realized that the above results and conclusions are based on a limited number of tests performed in the field on the steel and timber posts. Due to the limited time and resources available to the authors, repeatability of the tests was never verified. Dynamic field tests should also be conducted to verify the static test results.

RECOMMENDATIONS FOR FURTHER RESEARCH

The following areas are recommended for further research:

1. The conclusions drawn from this research study were based on a limited number of load tests conducted on steel and timber guardrail posts embedded with four different depths in two types of soil. To further support the findings of this study, additional load tests should be performed.
2. To verify the static load tests, dynamic field tests should be performed to study the dynamic behavior of guardrail posts under lateral loads.

REFERENCES

1. Broms, B., "Lateral Resistance of Piles in Cohesive Soils," Journal of Soil Mechanics and Foundations Division, ASCE, Vol. 90, No. SM2, March 1964, pp. 27-63.
2. Broms, B., "Lateral Resistance of Piles in Cohensionless Soils," Journal of Soil Mechanics and Foundations Division, ASCE, Vol. 90, No. SM3, March 1964, pp. 123-156.
3. Leps, Thomas M., "Review of Shearing Strength of Rockfill," Journal of Soil Mechanics and Foundation Division, ASCE, Vol. 96, No. SM4, July 1970, pp. 1157-1170.
4. Dewey, J. F., Jeyapalan, J. K., Hirsch, T. J., and Ross, H. E., "A Study of the Soil-Structure Interaction Behavior of Highway Guardrail Post," TTI Report No. 343-1 to SDHPT, Austin, Texas, July 1983.
5. Eggers, D. W., Hirsch, T. J., and Ross, H. E., "Strength of Guardrail Post in Rock," TTI Report No. 343-1 Supplement to SDHPT, Austin, Texas, September 1984.

APPENDIX A

SEQUENTIAL PHOTOGRAPHS FOR TESTS 5-16
(Tests 1-4 photographs are provided on colored slides)

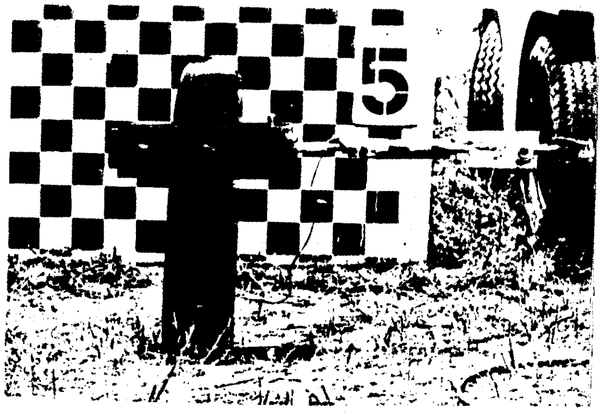

Deflection = 4.4 in.
Load = 1.3 k

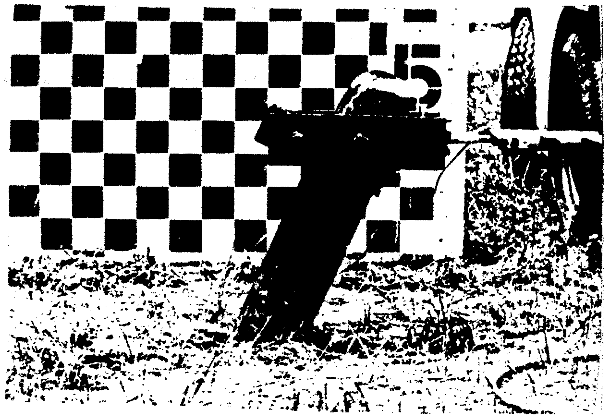

Deflection = 8.0 in.
Load = 1.05 k

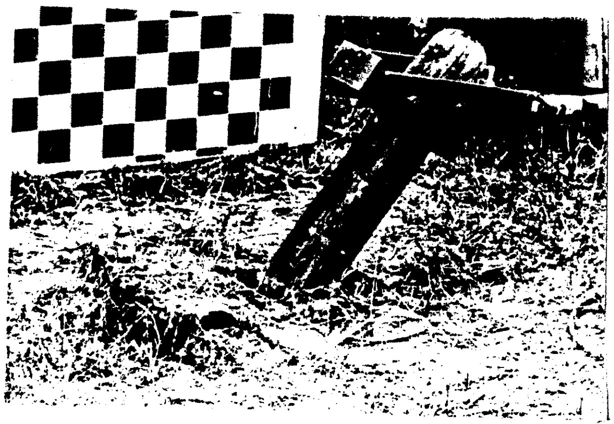

Deflection = 17.4 in.
Load = 0.74 k

FIG. 24.-Sequential Photographs for Test 5

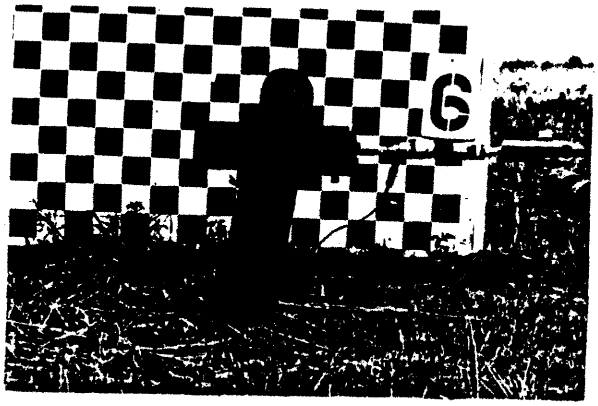

Deflection = 4.6 in.
Load = 1.8 k

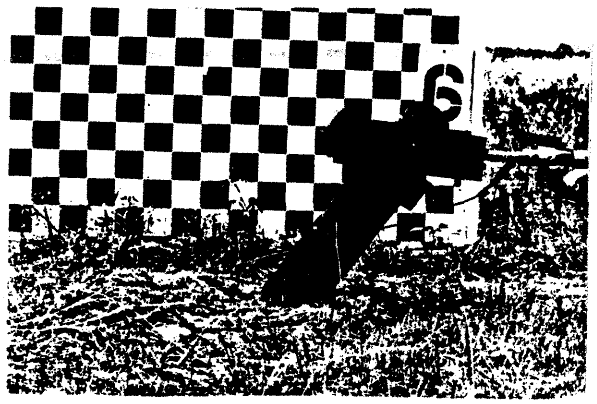

Deflection = 15.1 in.
Load = 2.13 k

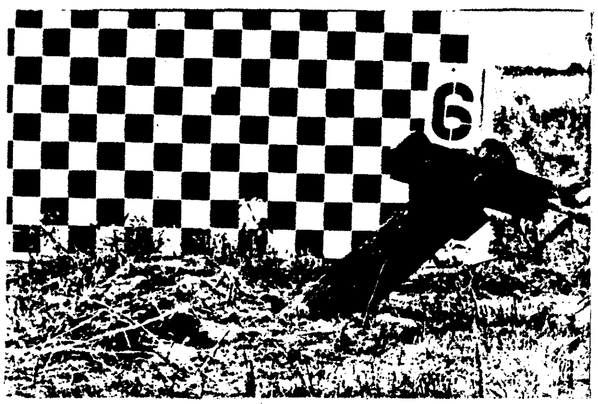

Deflection = 23.1 in.
Load = 1.32 k

FIG. 25.-Sequential Photographs for Test 6

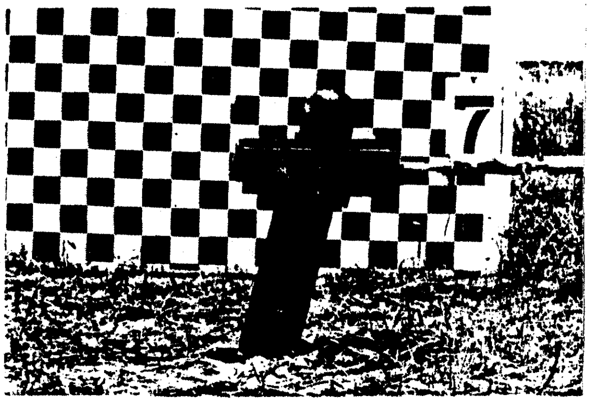

Deflection = 8.1 in.
Load = 2.03 k

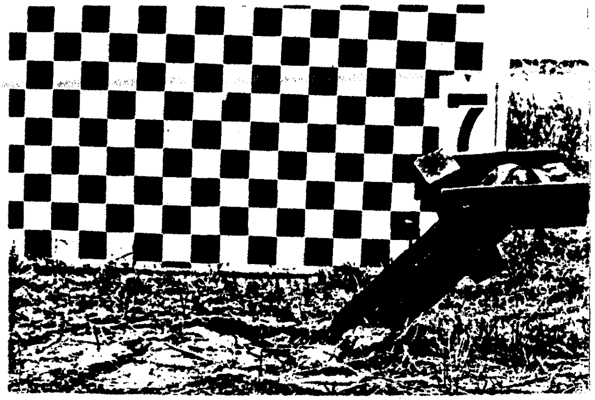

Deflection = 21.6 in.
Load = 3.07 k

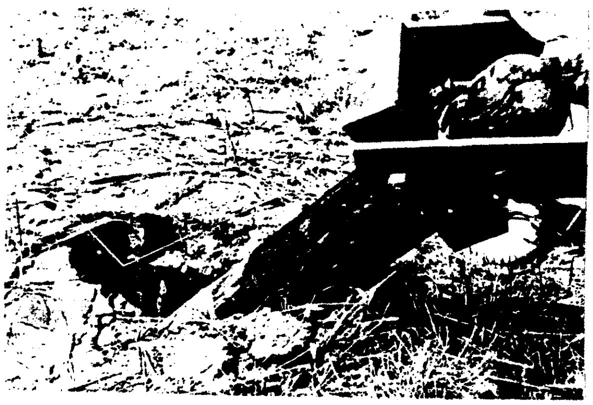

Deflection = 26.6 in.
Load = 3.2 k

FIG. 26.-Sequential Photographs for Test 7

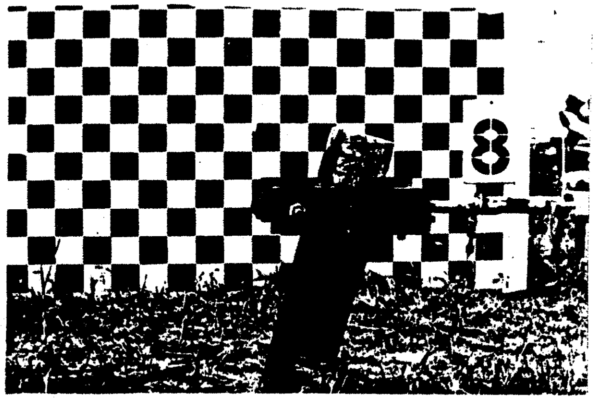

Deflection = 9.5 in.
Load = 2.75 k

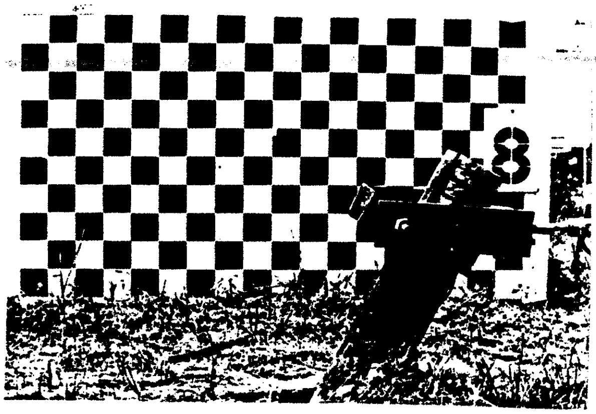

Deflection = 17.5 in.
Load = 4.07 k

Deflection = 29.0 in.
Load = 2.46 k

FIG. 27.-Sequential Photographs for Test 8

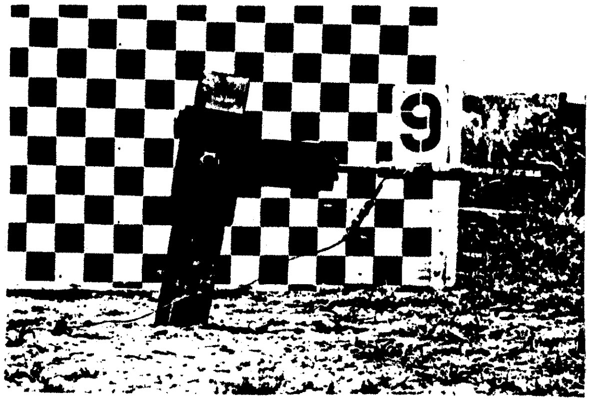

Deflection = 4.75 in.
Load = 0.43 k

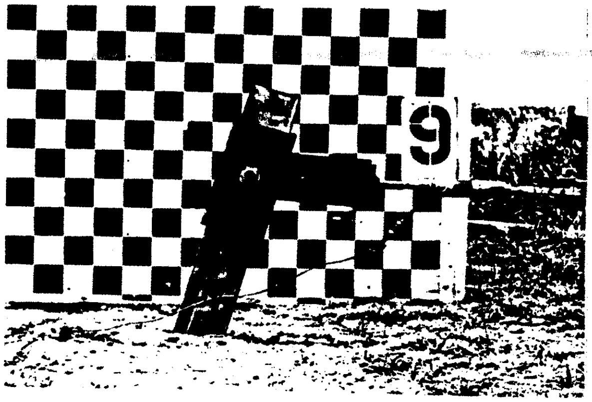

Deflection = 8.0 in.
Load = 0.18 k

Deflection = 12.5 in.
Load = 0.35 k

FIG. 28.-Sequential Photographs for Test 9

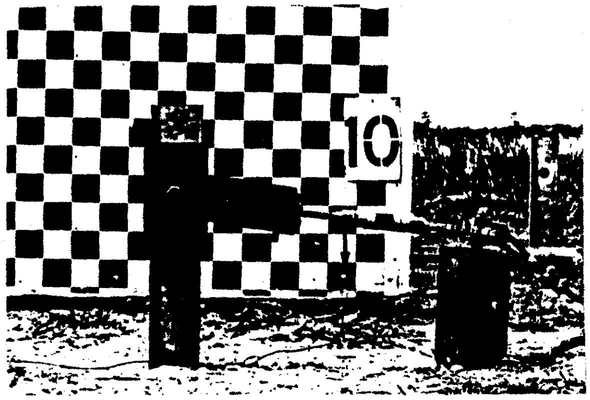

Deflection = 0.0 in.
Load = 0.0 k

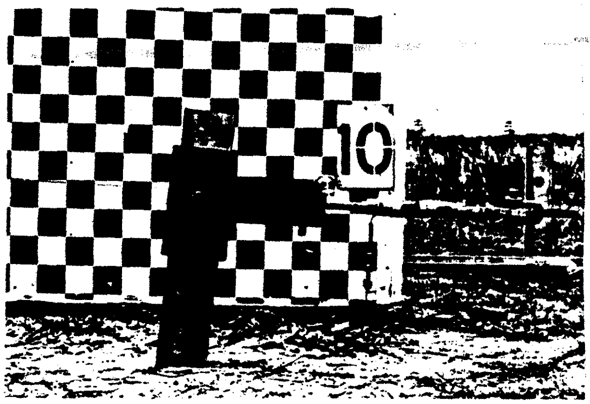

Deflection = 4.0 in.
Load = 1.1 k

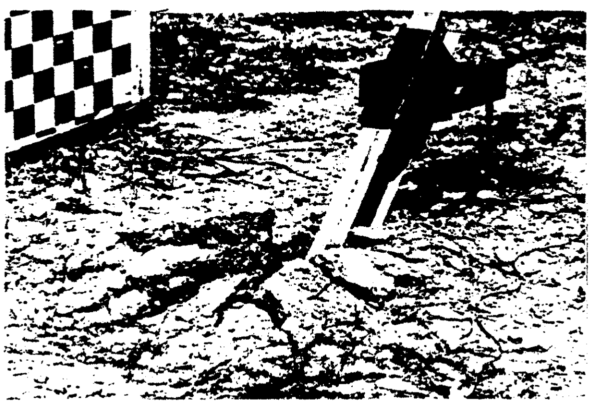

Deflection = 17.0 in.
Load = 0.19 k

FIG. 29.-Sequential Photographs for Test 10

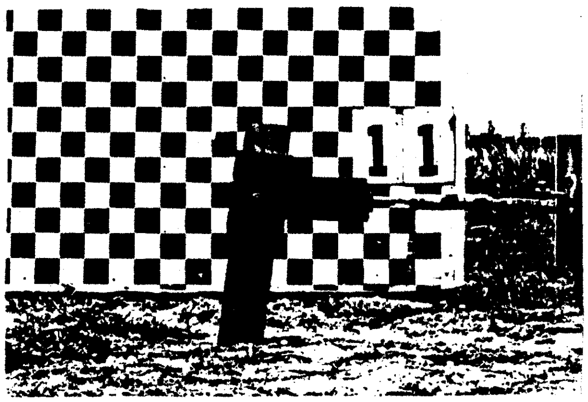

Deflection = 5.5 in.
Load = 2.16 k

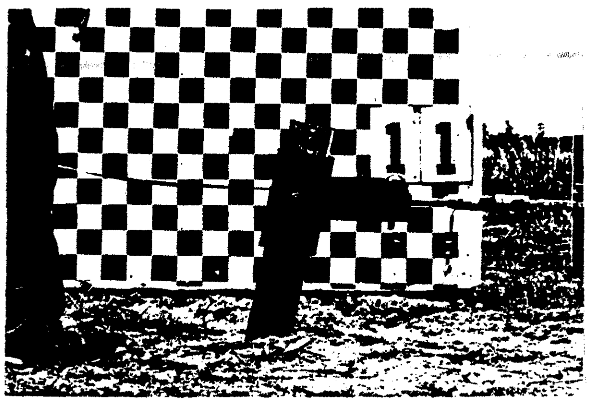

Deflection = 8.0 in.
Load = 2.4 k

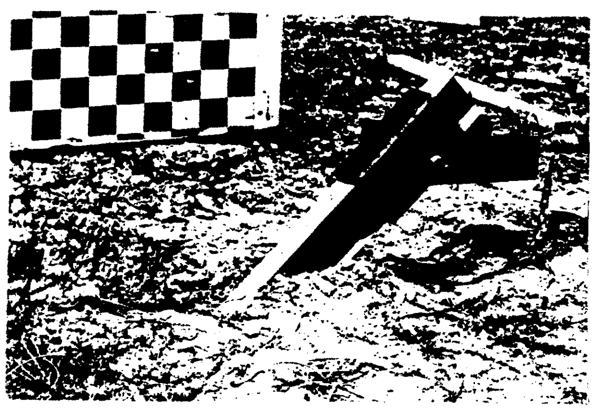

Deflection = 27.5 in.
Load = 0.41 k

FIG. 30.-Sequential Photographs for Test 11

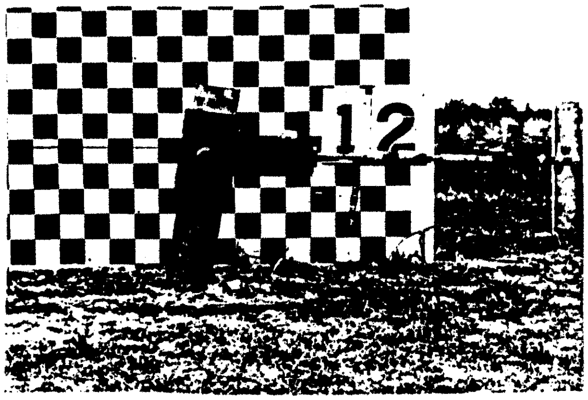

Deflection = 6.5 in.
Load = 3.89 k

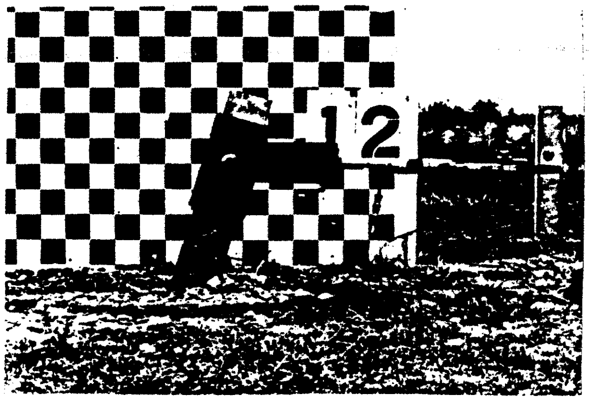

Deflection = 12.0 in.
Load = 4.66 k

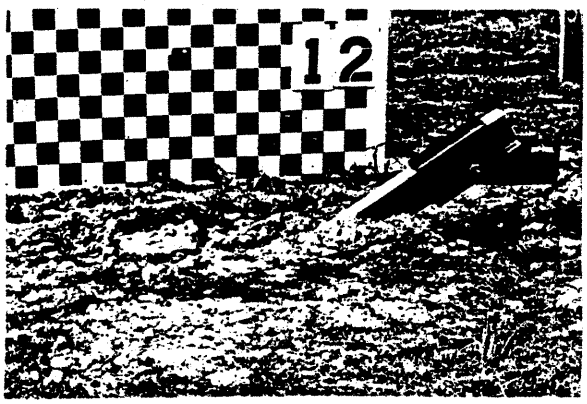

Deflection = 37.0 in
Load = 0.93

FIG. 31.-Sequential Photographs for Test 12

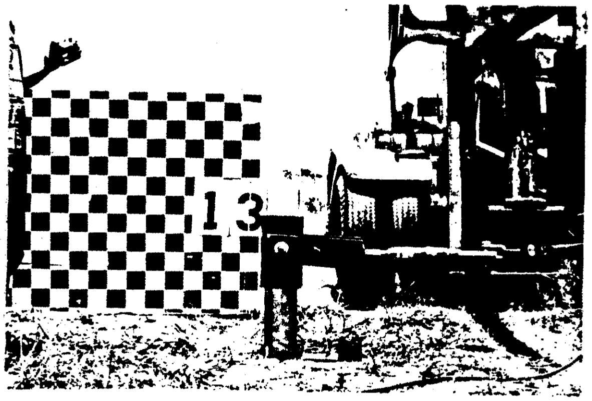

Deflection = 1.5 in.
Load = 0.84 k

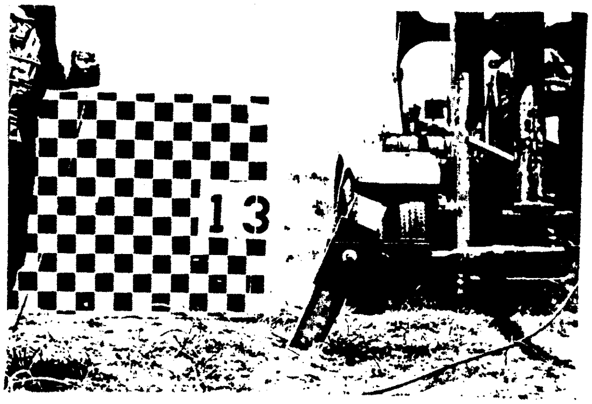

Deflection = 10.5 in.
Load = 0.38 k

Deflection = 12.5 in.
Load = 0.22 k

FIG. 32.-Sequential Photographs for Test 13

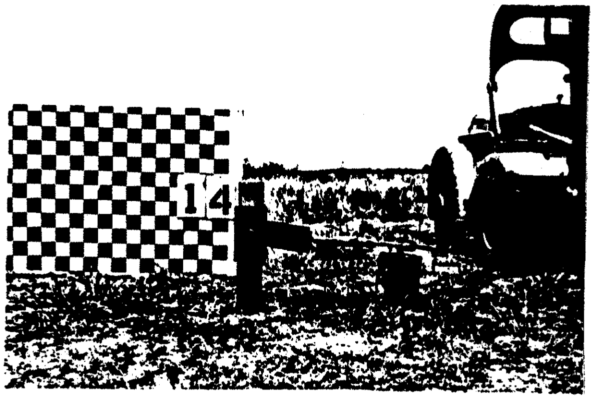

Deflection = 0.0 in
Load = 0.0 k

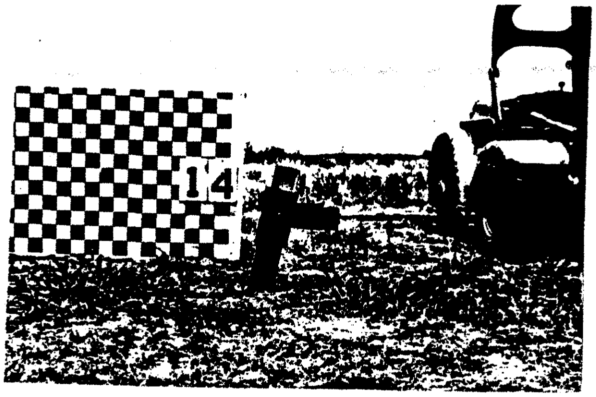

Deflection = 5.5 in.
Load = 1.15 k

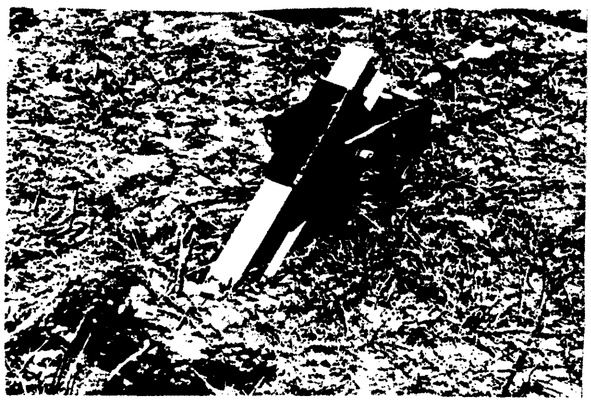

Deflection = 21.5 in.
Load = 0.25

FIG. 33.-Sequential Photographs for Test 14

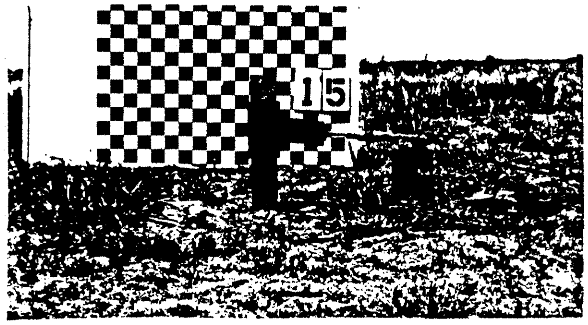

Deflection = 0.0 in.
Load = 0.0 k

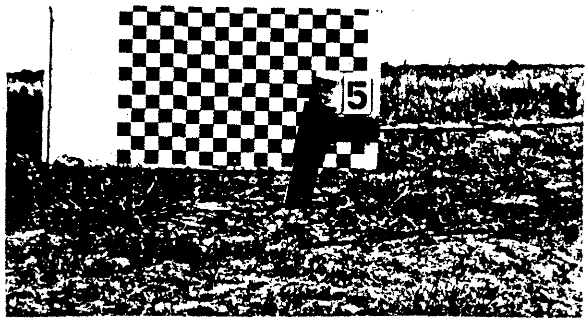

Deflection = 7.0 in.
Load = 1.85 k

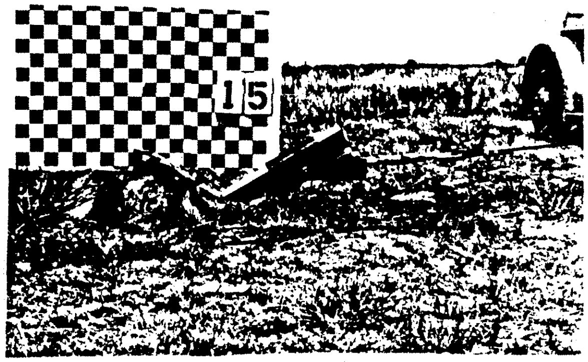

Deflection = 27.5 in.
Load = 0.39 k

FIG. 34.-Sequential Photographs for Test 15

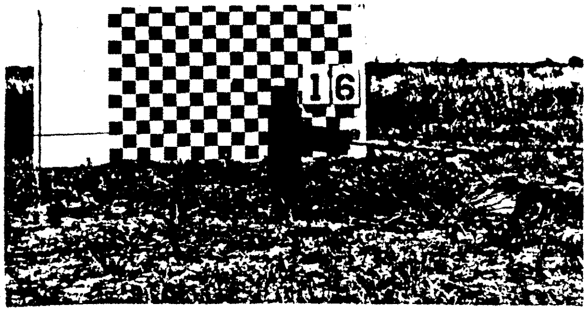

Deflection = 0.5 in.
Load = 0.73 k

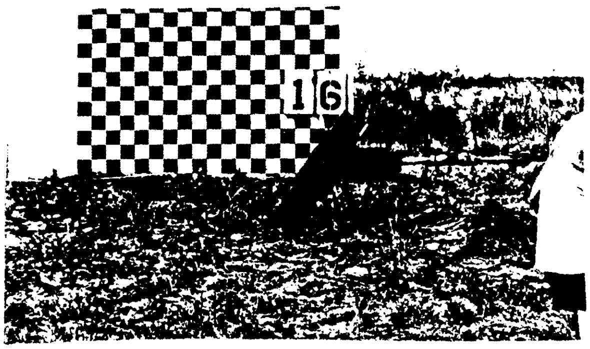

Deflection = 16.0 in
Load = 5.32 k

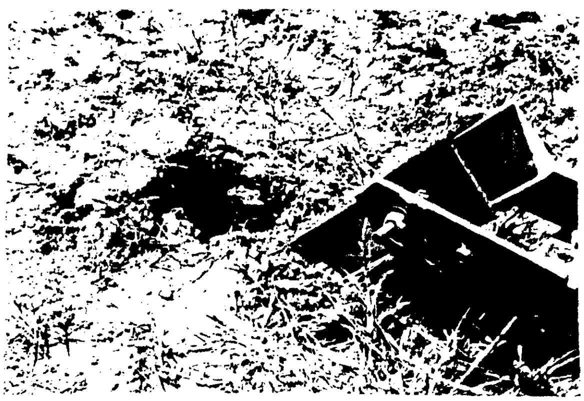

Deflection = 26.0 in.
Load = 5.6 k

FIG. 35.-Sequential Photographs for Test 16

APPENDIX B

SPECIFICATIONS FOR METAL BEAM GUARD FENCE

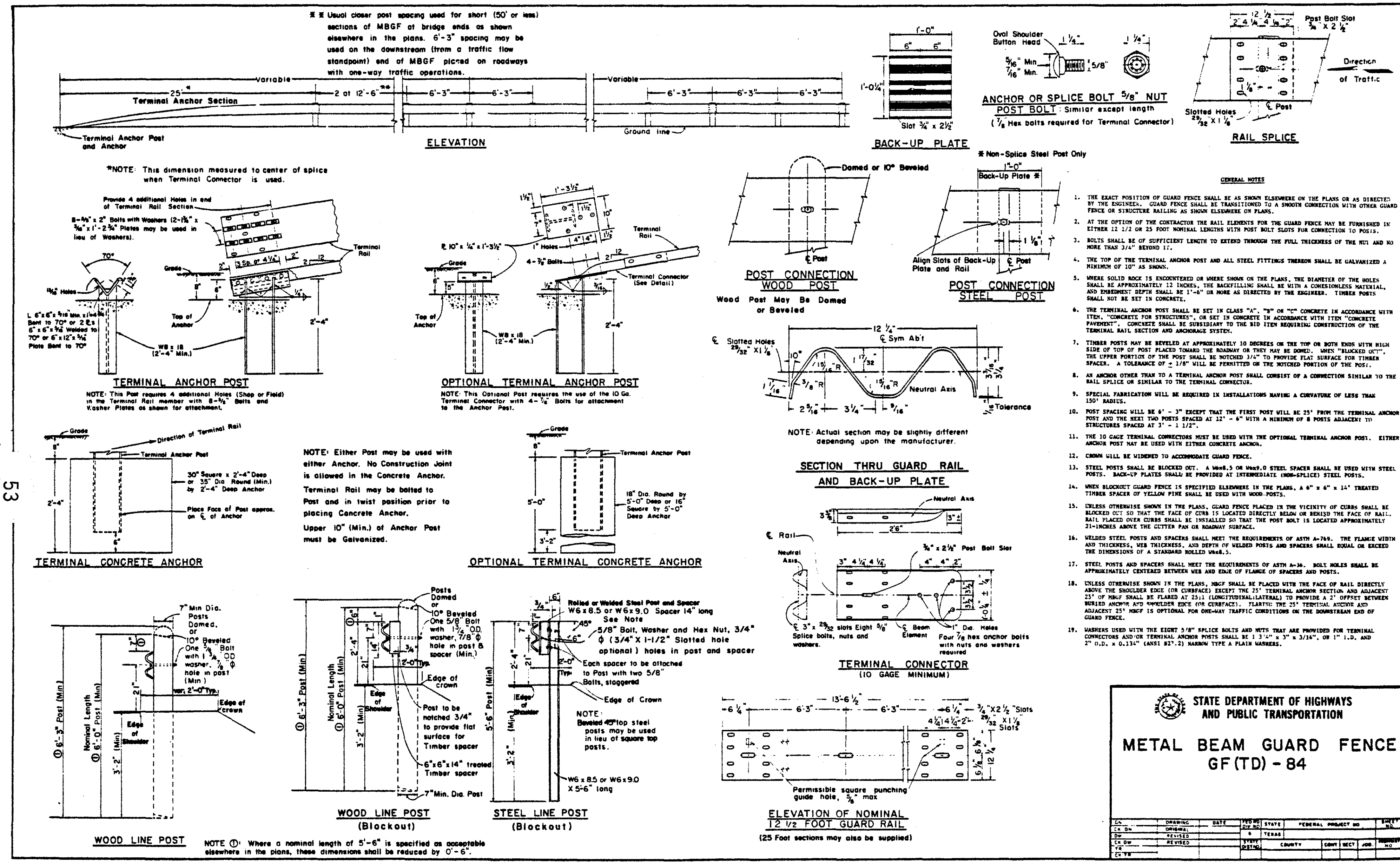

FIG. 36.-Specifications for Metal Beam Guard Fence